A trajectory-based estimate of the tropospheric ozone column using the residual method

M. R. Schoeberl,[1] J. R. Ziemke,[2] B. Bojkov,[2,3] N. Livesey,[4] B. Duncan,[2] S. Strahan,[2] L. Froidevaux,[4] S. Kulawik,[4] P. K. Bhartia,[1] S. Chandra,[2] P. F. Levelt,[5] J. C. Witte,[6] A. M. Thompson,[7] E. Cuevas,[8] A. Redondas,[8] D. W. Tarasick,[9] J. Davies,[9] G. Bodeker,[10] G. Hansen,[11] B. J. Johnson,[12] S. J. Oltmans,[12] H. Vömel,[13] M. Allaart,[5] H. Kelder,[5] M. Newchurch,[14] S. Godin-Beekmann,[15] G. Ancellet,[15] H. Claude,[16] S. B. Andersen,[17] E. Kyrö,[18] M. Parrondos,[19] M. Yela,[19] G. Zablocki,[20] D. Moore,[21] H. Dier,[22] P. von der Gathen,[23] P. Viatte,[24] R. Stübi,[24] B. Calpini,[24] P. Skrivankova,[25] V. Dorokhov,[26] H. de Backer,[27] F. J. Schmidlin,[28] G. Coetzee,[29] M. Fujiwara,[30] V. Thouret,[31] F. Posny,[32] G. Morris,[33] J. Merrill,[34] C. P. Leong,[35] G. Koenig-Langlo,[36] and E. Joseph[37]

Received 10 April 2007; revised 17 August 2007; accepted 12 September 2007; published 19 December 2007.

[1] We estimate the tropospheric column ozone using a forward trajectory model to increase the horizontal resolution of the Aura Microwave Limb Sounder (MLS) derived stratospheric column ozone. Subtracting the MLS stratospheric column from Ozone Monitoring Instrument total column measurements gives the trajectory enhanced tropospheric ozone residual (TTOR). Because of different tropopause definitions, we validate the basic residual technique by computing the 200-hPa-to-surface column and comparing it to the same product from ozonesondes and Tropospheric Emission Spectrometer measurements. Comparisons show good agreement in the tropics and reasonable agreement at middle latitudes, but there is a persistent low bias in the TTOR that may be due to a slight high bias in MLS stratospheric column. With the improved stratospheric column resolution, we note a strong correlation of extratropical tropospheric ozone column anomalies with probable troposphere-stratosphere exchange events or folds. The folds can be identified by their colocation with strong horizontal tropopause gradients. TTOR anomalies due to folds may be mistaken for pollution events since folds often occur in the Atlantic and Pacific pollution corridors. We also compare the 200-hPa-to-surface

[1]NASA Goddard Space Flight Center, Greenbelt, Maryland, USA.
[2]Goddard Earth Sciences and Technology, University of Maryland, Baltimore County, Baltimore, Maryland, USA.
[3]Also at NASA Goddard Space Flight Center, Greenbelt, Maryland, USA.
[4]NASA Jet Propulsion Laboratory, Pasadena, California, USA.
[5]Royal Netherlands Meteorological Institute, De Bilt, Netherlands.
[6]Science Systems and Applications Inc., Lanham, Maryland, USA.
[7]Department of Meteorology, Pennsylvania State University, University Park, Pennsylvania, USA.
[8]Izana Observatory, National Institute of Meteorology, Santa Cruz de Tenerife, Spain.
[9]Environment Canada, Downsview, Ontario, Canada.
[10]National Institute of Water and Atmospheric Research, Lauder, New Zealand.
[11]Norwegian Institute for Air Research, Tromso, Norway.
[12]Global Monitoring Division, Earth System Research Laboratory, NOAA, Boulder, Colorado, USA.
[13]Cooperative Institute for Research in Environmental Sciences, University of Colorado, Boulder, Colorado, USA.
[14]Atmospheric Science Department, University of Alabama-Huntsville, Huntsville, Alabama, USA.
[15]Service d'Aeronomie, Centre National de la Recherche Scientifique/Université Pierre et Marie Curie, Paris, France.
[16]Meteorological Observatory Hohenpeißenberg, German Weather Service, Hohenpeißenberg, Germany.
[17]Danish Meteorological Institute, Copenhagen, Denmark.
[18]Arctic Research Center, Finish Meteorological Institute, Sodankyla, Finland.
[19]Laboratorio de Atmosfera, Spanish Space Agency, Madrid, Spain.
[20]Centre of Aerology, National Institute of Meteorology and Hydrology, Legionowo, Poland.
[21]Met Office, Exeter, UK.
[22]Meteorological Observatory Lindenberg, German Weather Service, Lindenberg, Germany.
[23]Alfred Wegener Institute, Potsdam, Germany.
[24]Aerological Station Payerne, MeteoSwiss, Payerne, Switzerland.
[25]Czech Hydrometeorological Institute, Prague, Czech Republic.
[26]Central Aerological Observatory, Moscow, Russia.
[27]Royal Meteorological Institute of Belgium, Uccle, Belgium.
[28]NASA Goddard Space Flight Center, Wallops Island, Virginia, USA.
[29]Department of Environmental Affairs and Tourism, South African Weather Service, Pretoria, South Africa.
[30]Graduate School of Environmental Earth Science, Hokkaido University, Sapporo, Japan.
[31]Laboratoire d'Aerologie, CNRS, Toulouse, France.
[32]Laboratoire de Physique de l'Atmosphere de la Reunion, La Reunion, France.
[33]Department of Physics and Astronomy, Valparaiso University, Valparaiso, Indiana, USA.
[34]Graduate School of Oceanography, University of Rhode Island, Narragansett, Rhode Island, USA.
[35]Malaysian Meteorological Service, Jalan Sultan, Selangor, Malaysia.
[36]Alfred Wegener Institute, Bremerhaven, Germany.
[37]Climate and Radiation Group, Howard University, Washington, D. C., USA.

Copyright 2007 by the American Geophysical Union.
0148-0227/07/2007JD008773

column with Global Modeling Initiative chemical model estimates of the same quantity. While the tropical comparisons are good, we note that chemical model variations in 200-hPa-to-surface column at middle latitudes are much smaller than seen in the TTOR.

Citation: Schoeberl, M. R., et al. (2007), A trajectory-based estimate of the tropospheric ozone column using the residual method, *J. Geophys. Res.*, *112*, D24S49, doi:10.1029/2007JD008773.

1. Introduction

[2] The tropospheric column ozone residual method estimates the tropospheric column ozone by subtracting measurements of stratospheric ozone column from total column ozone. The tropospheric ozone column rarely exceeds 80 DU and thus is always a smaller component of the total ozone column (~250–500 DU). Total ozone column has been accurately measured by the Total Ozone Mapping Spectrometer instrument series starting in late 1978 and most recently the Dutch-Finnish Ozone Monitoring Instrument (OMI) [*Levelt et al.*, 2006] on Aura. Although tropospheric ozone can be estimated directly using UV instruments [e.g., *Liu et al.*, 2006], we focus on the residual technique because, in theory, it can produce a more precise tropospheric column. The key to producing the tropospheric column is an accurate estimation of the larger stratospheric ozone column. Various instruments have been used to derive the stratospheric column including Stratospheric Aerosol and Gas Experiment II [*Fishman and Larsen*, 1987; *Fishman et al.*, 1990], Upper Atmosphere Research Satellite (UARS) Microwave Limb Sounder (MLS) [*Chandra et al.*, 2003] and Aura's Earth Observing System MLS [*Ziemke et al.*, 2006, hereinafter referred to as Z06]. Up until the launch of Aura and ENVISAT, near simultaneous stratospheric column and total column ozone amounts were not available. A brief review of tropospheric ozone residual techniques is given in Z06 and is not repeated here.

[3] The Aura MLS instrument [*Waters et al.*, 2006] can be used to estimate the stratospheric column as in Z06. One advantage of the Aura MLS over the previous UARS MLS instrument is that Aura MLS was designed to retrieve ozone in the lower stratosphere and upper troposphere (UTLS). The second advantage is that because Aura is in a Sun-synchronous orbit, Aura MLS instrument can produce near global maps of stratospheric column on a daily basis. The OMI and MLS instruments onboard the Aura spacecraft have been providing global measurements of total column ozone and stratospheric column soon after the launch of Aura on 15 July 2004 [*Schoeberl et al.*, 2006]. This has enabled near global estimates of the tropospheric column on almost a day-to-day basis from late September 2004 to present.

[4] In Z06, Aura MLS stratospheric column and OMI total column ozone data were used to produce a monthly mean and daily tropospheric ozone residual. However, with only ~14.6 orbits a day, the MLS ascending node (daytime) measurements of stratospheric column provide only a low horizontal resolution mapped product (~24.7° longitude by ~2° latitude). The interpolation of MLS data onto the OMI grid to generate the residual, implicitly forces smaller-scale variability seen in the OMI total column ozone to be part of the tropospheric column. This assumption probably does not strongly affect the computation of the monthly mean residual because the smaller-scale variability will average out in a month. Indeed, Z06 showed that monthly mean sonde profiles were consistent with residual estimates from ozonesondes. However, the Z06 method does not produce a reasonable extratropical product as judged by sonde comparison (shown below). We hypothesize that the main problem is that the approach used by Z06 has to be modified to account for stratospheric column spatial variability.

[5] In this study, we use forward trajectory calculations to boost the horizontal resolution of the stratospheric column, and this allows us to generate an improved daily tropospheric ozone residual. In the next section, we describe the data and method. We validate our results with daily ozonesondes. We also compare the data with Tropospheric Emission Spectrometer (TES) [*Beer*, 2006] direct estimates of the ozone column. We show some examples of tropospheric enhancements near tropopause folds: midlatitude synoptic-scale features often associated with jumps in the tropopause height along jets and cutoff low pressure systems. These jumps are often colocated with changes in column ozone and water vapor and can be diagnosed from satellite data [*Wimmers and Moody*, 2004]. The fold enhancements in ozone are clearly present in the observations. Finally we show how our estimates of the tropospheric column compare with NASA Global Modeling Initiative (GMI) estimates of the column (see Z06).

2. Overview of Method

[6] OMI is a nadir-scanning instrument that detects backscattered solar radiance to measure column ozone. OMI pixels have a nadir resolution of 13 km × 24 km [*Levelt et al.*, 2006]. Total ozone from OMI is derived using the Total Ozone Mapping Spectrometer version 8 algorithm [*Bhartia*, 2007].

[7] The Aura MLS instrument measures vertical profiles of mesospheric, stratospheric, and upper tropospheric temperature, ozone and other constituents from limb scans. The MLS profile measurements are taken about 7 min before OMI views the same location during daytime orbital tracks. Details regarding the instrument including spectrometers, spectral channels, calibration, and other topics are discussed by *Waters et al.* [2006]. *Froidevaux et al.* [2006] and *Livesey et al.* [2007] provide validation results on the Aura MLS algorithm version 1.5 and version 2.2 measurements of ozone and other constituents; version 1.5 is used here because of insufficient version 2.2 data.

[8] About two and a half years of ozone data have been archived as level 2GP for MLS and level 2 gridded (L2G), and level-3 (L3) for OMI beginning in September 2004. Z06 use the OMI L3 and MLS L2 (ascending node only) data to produce maps of stratospheric column and the residual. In Z06, stratospheric column is generated by interpolating between MLS measurement points that are ~24.7° in longitude apart. This approach assigns the

21562202d, 2007, D24, Downloaded from https://agupubs.onlinelibrary.wiley.com/doi/10.1029/2007JD008773 by Spanish Cochrane National Provision (Ministerio de Sanidad), Wiley Online Library on [22/01/2026]. See the Terms and Conditions (https://onlinelibrary.wiley.com/terms-and-conditions) on Wiley Online Library for rules of use; OA articles are governed by the applicable Creative Commons License

smaller-scale variability of the stratospheric column to the tropospheric column. Increasing the resolution of the stratospheric column map would improve the tropospheric column estimate. There are at least three approaches to increasing the stratospheric column resolution: (1) MLS data can be trajectory mapped [*Morris et al.*, 2000] to form a higher-resolution field; (2) MLS ozone can be PV mapped assuming that there is a high correlation between PV and ozone in the lower stratosphere, PV becomes a surrogate for ozone (Q. Yang et al., Midlatitude tropospheric ozone columns derived from the Aura Ozone Monitoring Instrument and the Microwave Limb Sounder measurements, submitted to *Journal of Geophysical Research*, 2007); and (3) MLS data can be assimilated in a 3-D chemical model (see I. Stajner et al., Assimilated ozone from EOS-Aura: Evaluation of the tropopause region and tropospheric columns, submitted to *Journal of Geophysical Research*, 2007, hereinafter referred to as Stajner et al., submitted manuscript, 2007). In this study we take the former approach. Yang et al. show that PV mapping also improves the midlatitude TOR estimates but will likely fail where PV-ozone correlations break down. Full 3-D chemical assimilation (albeit computationally expensive) is probably the ultimate solution since modern assimilation techniques better handle instrumental and meteorological measurement uncertainties.

[9] MLS L2 is provided at the position of the satellite maps. We use only data that has been flagged as acceptable quality. Occasionally, the MLS algorithm will fail to converge for a profile and that profile is flagged. We interpolate along the MLS track and replace the flagged profile with an interpolated profile from near by points. If more than five sequential profiles are data are flagged, no interpolation is performed.

[10] The trajectory mapping approach is to simply move the measurement made at one time to another time using the trajectory model and assimilated meteorological data. We used only forward mapping here. (*Morris et al.* [2000] used both forward and backward mapping.) MLS ozone profiles precision percentage uncertainty increases moving from the stratosphere downward into the upper troposphere. Measurements at pressures above about 215 hPa (near the midlatitude tropopause) are probably not accurate enough for our purposes. Since we wish to avoid data from pressure above 215 hPa produced by backward trajectories ascending into the midlatitude stratosphere we restrict ourselves to forward trajectory mapping. The ascent of air from above 215 hPa into the stratosphere is not as much of a concern in the tropics because the ascent is slow and the 215 hPa level is well below the tropopause.

[11] The 6 d of forward trajectories from both day and night MLS observations are accumulated for each analysis day (target day). Our experience with trajectory calculations at these altitudes suggests that 6 d is the practical time limit for such mapping due to the accumulation of errors associated with the meteorological fields [*Schoeberl and Sparling*, 1995]. The trajectories are isentropic. For the target day, only the ascending node (daytime) MLS data are used because those data correspond to OMI measurements taken on the same day. The meteorological fields used to drive the trajectory model are the GEOS-4 winds and temperatures [*Bloom et al.*, 2005]. Experiments with the technique show that we only need to trajectory map data below 10 hPa and we can use the Z06 spatial interpolation approach for higher altitudes. Thus each MLS pressure level between 215 hPa and 10 hPa is trajectory mapped. After the data are mapped all of the points are remapped onto the GEOS-4 grid using linear interpolation. To summarize, the procedure to generate the stratospheric column is as follows: First, the MLS measurements are screened using the recommended quality flags then the data are interpolated along the MLS track to fill in any missing values. Using the trajectory code, up to 6 d of measurements points between 215 hPa and 10 hPa are isentropically moved forward to a target time. If a trajectory descends below 215 hPa it is removed. At the target time, the MLS ozone data are interpolated onto a map at the GEOS-4 resolution, $1^\circ \times 1.25^\circ$ (latitude, longitude) at the MLS L2 pressure levels.

[12] Figure 1 (top) shows the trajectory locations for points accumulated over the last 6 d and the actual measurements points for MLS on 24 June 2005 on the 100 hPa surface only. (Other surfaces are also trajectory mapped but not shown for illustration purposes.) It is evident that the forward trajectory mapping significantly increases the amount of data that can be used in generating the stratospheric column map. Note however, that there are still gaps and we will have to interpolate to fill in the gaps. Nonetheless there is significantly more information available for the interpolation than with a single day's MLS data.

[13] Figure 1 (middle) also shows that the increase in data through the forward trajectory system does not produce large-scale changes in the stratospheric column, but it does produce subtle changes in the smaller-scale features. One additional advantage of the trajectory scheme is that if the MLS instrument is not taking data on a particular day we can use the data from previous days to generate the stratospheric column.

[14] After generating the stratospheric column, the OMI total column (see the OMI Algorithm Theoretical Basis Document, http://toms.gsfc.nasa.gov/version8/v8toms_atbd.pdf) measurements are screened via the recommended L2 data quality flags. We use OMI L2G data interpolated to the GEOS-4 grid. Total ozone data are further screened using the reflectivity: Scenes with reflectivity greater than 0.6 are considered cloudy and are not used (1.0 reflectivity is fully cloud covered); Z06 screened data based on 0.3 reflectivity but in our comparisons below the Z06 product is screened for 0.6. In fully cloudy cases, the ozone algorithm uses climatological tropospheric ozone, but even with 0.6 reflectivity, some residual information on the tropospheric ozone is in the data.

[15] Finally, to compute the residual the tropopause pressure is required. For this study we use the following algorithm for the tropopause: the tropopause is the lowest of

Figure 1. (top) Low-resolution tropospheric ozone with MLS measurement points on the target day (black) and forward trajectory points (white) from MLS measurements using the last 6 d of data. (middle) Same without measurement points. In Figure 1 (top and middle) only MLS data from the black measurement points are used. (bottom) High-resolution stratospheric column using all the points shown in Figure 1 (top).

21562202d, 2007, D24, Downloaded from https://agupubs.onlinelibrary.wiley.com/doi/10.1029/2007JD008773 by Spanish Cochrane National Provision (Ministerio de Sanidad), Wiley Online Library on [22/01/2026]. See the Terms and Conditions (https://onlinelibrary.wiley.com/terms-and-conditions) on Wiley Online Library for rules of use; OA articles are governed by the applicable Creative Commons License

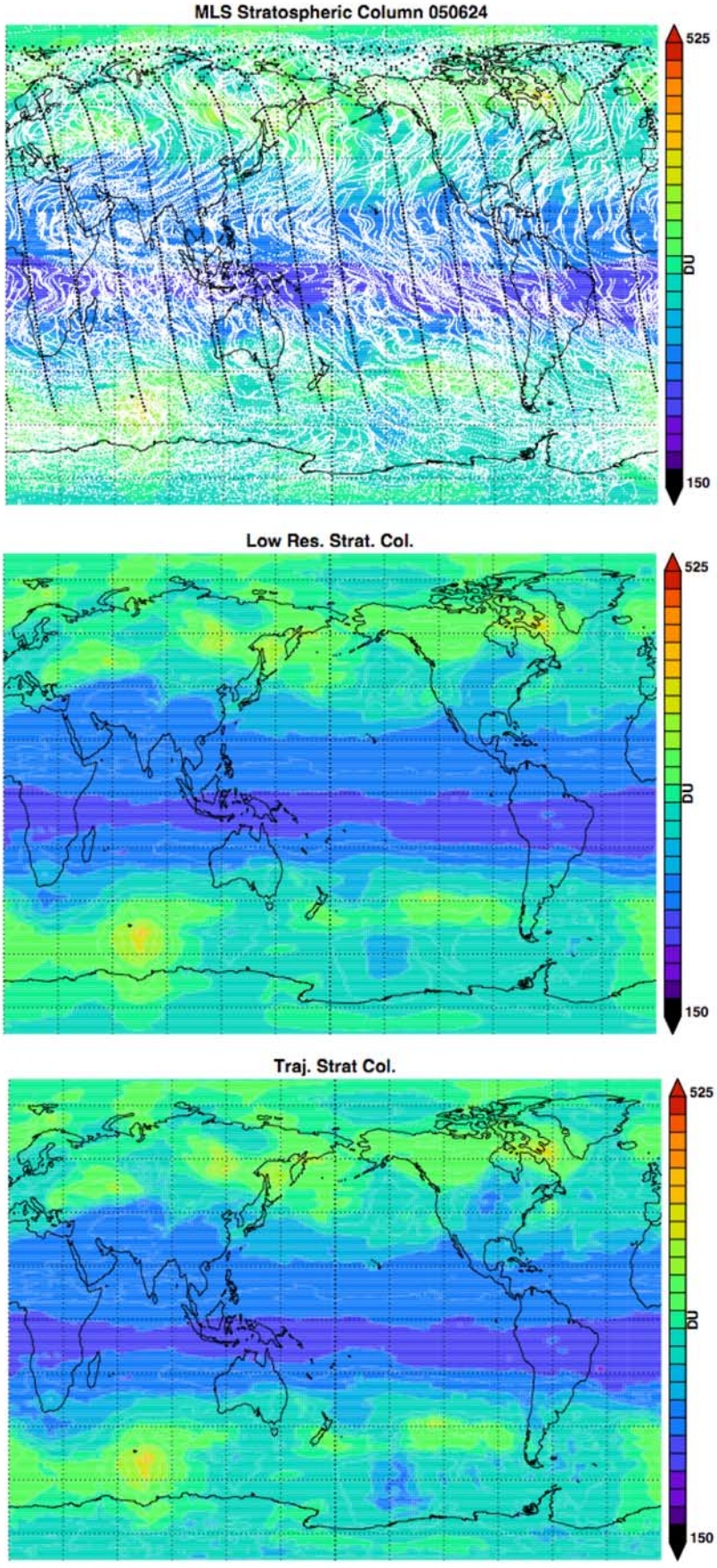


Figure 1

21562202d, 2007, D24, Downloaded from https://agupubs.onlinelibrary.wiley.com/doi/10.1029/2007JD008773 by Spanish Cochrane National Provision (Ministerio de Sanidad), Wiley Online Library on [22/01/2026]. See the Terms and Conditions (https://onlinelibrary.wiley.com/terms-and-conditions) on Wiley Online Library for rules of use; OA articles are governed by the applicable Creative Commons License

the following, the |3.5| PVU surface, the <2 K km^{-1} surface (or approximately World Meteorological Organization lapse rate tropopause), the cold point tropopause, the 380 K surface. Generally, the PV tropopause is the lower than the lapse rate tropopause except in the tropics [*Schoeberl*, 2004; Stajner et al., submitted manuscript, 2007]. In the tropics, the lapse rate and cold point tropopause coincide and are rarely above 380 K. Choosing the lowest tropopause from the ensemble avoids the complexity that arises when there is a double tropopause [*Randel et al.*, 2007]. Z06 uses the lapse rate tropopause from NCEP analyses. The different tropopause definitions between analyses creates biases between various computations of the residual. Even if the same tropopause definition is used, biases can arise between sondes and global models because the later provide the average tropopause height over a grid box as opposed to sondes which provide a local tropopause height. Thus, in the validation section below we use a 200-hPa-to-surface column (200TSC) which removes tropopause pressure level produced biases.

[16] We generate the residual by subtraction of the stratospheric column from the OMI total ozone column. The OMI and MLS data are not synoptic, that is, the measurement times vary with global location. To generate asynoptic stratospheric column to match the OMI data, the MLS data are forward trajectory transported to the asynoptic times of the OMI data. The tropopause pressure is also time interpolated from the four GEOS-4 synoptic times to the asynoptic OMI total column. Although this is a much more complicated scheme than simply assuming (as in Z06 and previous studies) that the OMI and MLS fields are synoptic (or time simultaneous), we find that if the asynoptic nature of the data are not considered, tropopause fold anomalies can be significantly overestimated or underestimated. Finally, during the course of our computations we generate a quality flag which indicates points with high reflectivity (>0.6), anomalous total column ozone (column below 100 DU), low tropopause (below 200 hPa), OMI L2 flags (such as missing data) or other problems. All of the validation calculations discussed below are made with high-quality data (no flags).

[17] Between any two pressure levels the ozone column in Dobson Units (DU) is

$$ColO_3 = 0.7889 \int_{p_{top}}^{p_{bottom}} \mu dp \qquad (1)$$

[*Dessler*, 2005] where μ is ozone volume mixing ratio in units ppbv and p is pressure (p_{top} is the lower pressure) in hPa. If we know both the tropopause and surface pressure, we can compute the tropospheric average mixing ratio that would generate the tropospheric column residual. The principal advantage of the tropospheric average mixing ratio is that surface pressure changes due to weather or topography that influence the column are removed.

[18] Figure 2 shows an example of the fields that are combined with the stratospheric column to generate the tropospheric column at the GEOS-4 resolution. Figure 2 (top) shows the OMI column. We focus our attention on the region of high tropospheric ozone off the east coast of North America. The tropopause height plot (Figure 2, middle) shows us that there is a strong east-west gradient in that region which is one of the characteristics of a tropopause folding event. The magnitude of the tropopause gradient is contoured in black (units are unimportant). Elsewhere on the map high OMI column amounts are often colocated with the strong east-west tropopause gradients. The residual also shows high values on the cyclonic side of the jet expected with a stratosphere-troposphere exchange event. This gives us confidence that the residual captures at least some of the daily variability. Stajner et al. (submitted manuscript, 2007) also note high tropospheric column events on the cyclonic side of the jet in their assimilated tropospheric column. The tropopause ozone gradient is a key factor in interpreting daily results. High, localized tropospheric column events off the east coast of the United States or China that might appear to be pollution events are often folds. In the rest of this paper we refer to residual products produced using the trajectory method of estimating stratospheric column as trajectory enhanced tropospheric ozone residual (TTOR).

3. Validation of OMI/MLS Tropospheric and Stratospheric Ozone Measurements

[19] *Froidevaux et al.* [2006] discuss MLS ozone validation. The V1.5 MLS ozone profiles evaluated for 0.46–215 hPa tend to be within about 1% of column amounts calculated from SAGE II, but MLS tends to overestimate ozone in the very lower part of the stratosphere by up to 20% compared to SAGE II and POAM data. The newest version of the MLS algorithm, V2.2, show improvements in lower stratospheric ozone retrievals (L. Froidevaux et al., Validation of Aura Microwave Limb Sounder stratospheric ozone measurements, submitted to *Journal of Geophysical Research*, 2007), but too little V2.2 MLS data has been processed using the newest algorithm to use it here.

[20] OMI total ozone measurements have been extensively validated with both ground-based Brewer and Dobson data, Earth Probe Total Ozone Mapping Spectrometer data, and Solar Backscatter Ultraviolet/2 data. Comparisons between OMI and ground-based total column ozone measurements indicates that OMI column ozone is within ~1% of the ground-based measurements (R. D. McPeters et al., Validation of the total column ozone data product of the Ozone Monitoring Instrument aboard NASA EOS-Aura, submitted to *Journal of Geophysical Research*, 2007, hereinafter referred to as McPeters et al., submitted manuscript, 2007). To summarize, the MLS stratospheric column may be slightly high biased by a few DU, and if the OMI column has almost no bias, the TTOR will be low biased.

3.1. Sonde Validation of the 200 hPa to Surface Column

[21] Z06 discussed comparisons of their tropospheric ozone residual product with ozonesonde estimates of the

Figure 2. (top) OMI column ozone field in DU for 24 June 2005. (middle) Tropopause height in km. Black contours show the amplitude of the tropopause gradient. (bottom) Tropospheric ozone residual in DU. Crosses indicate points where the quality flag indicates issues with the calculation such as no column measurement, low tropopause or high reflectivity.

21562202d, 2007, D24, Downloaded from https://agupubs.onlinelibrary.wiley.com/doi/10.1029/2007JD008773 by Spanish Cochrane National Provision (Ministerio de Sanidad), Wiley Online Library on [22/01/2026]. See the Terms and Conditions (https://onlinelibrary.wiley.com/terms-and-conditions) on Wiley Online Library for rules of use; OA articles are governed by the applicable Creative Commons License

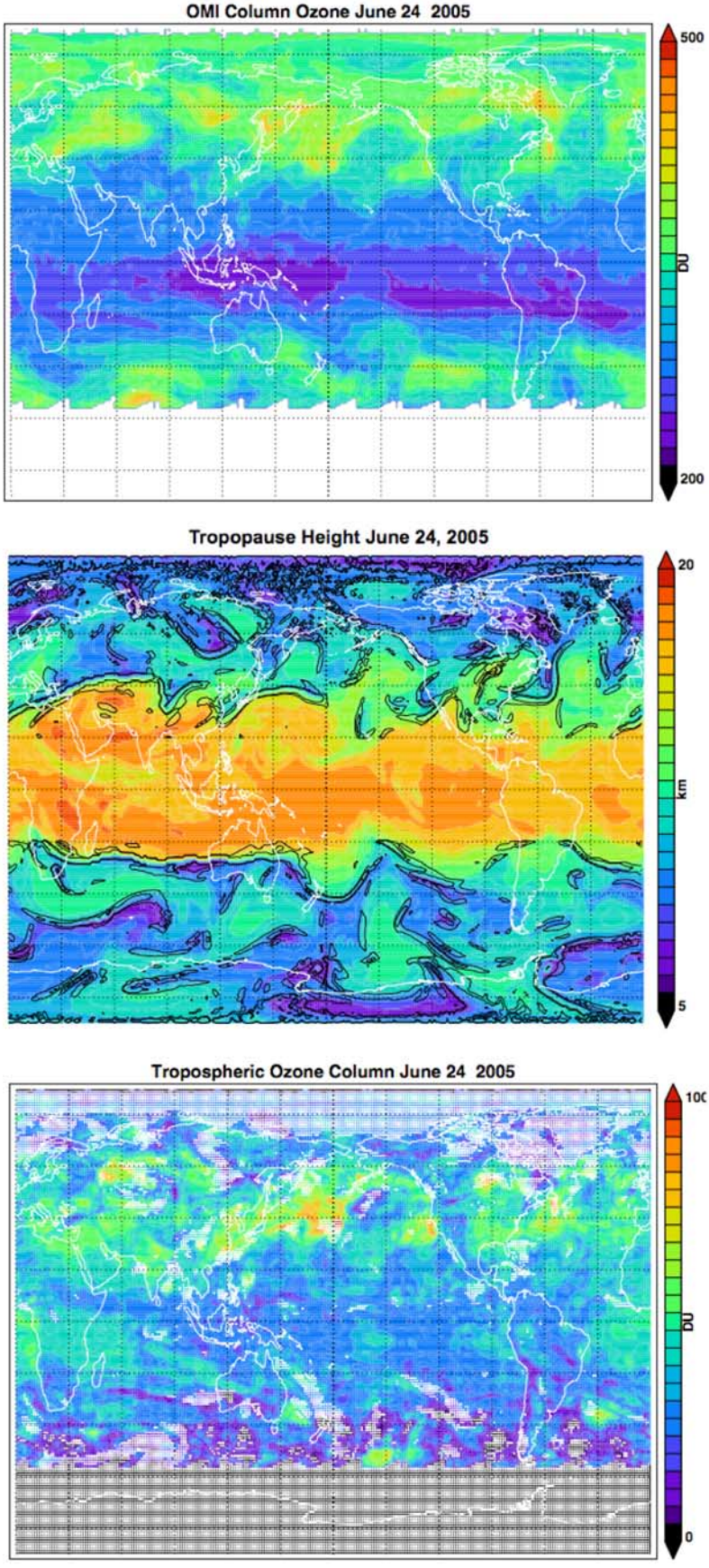


Figure 2

21562202d, 2007, D24, Downloaded from https://agupubs.onlinelibrary.wiley.com/doi/10.1029/2007JD008773 by Spanish Cochrane National Provision (Ministerio de Sanidad), Wiley Online Library on [22/01/2026]. See the Terms and Conditions (https://onlinelibrary.wiley.com/terms-and-conditions) on Wiley Online Library for rules of use; OA articles are governed by the applicable Creative Commons License

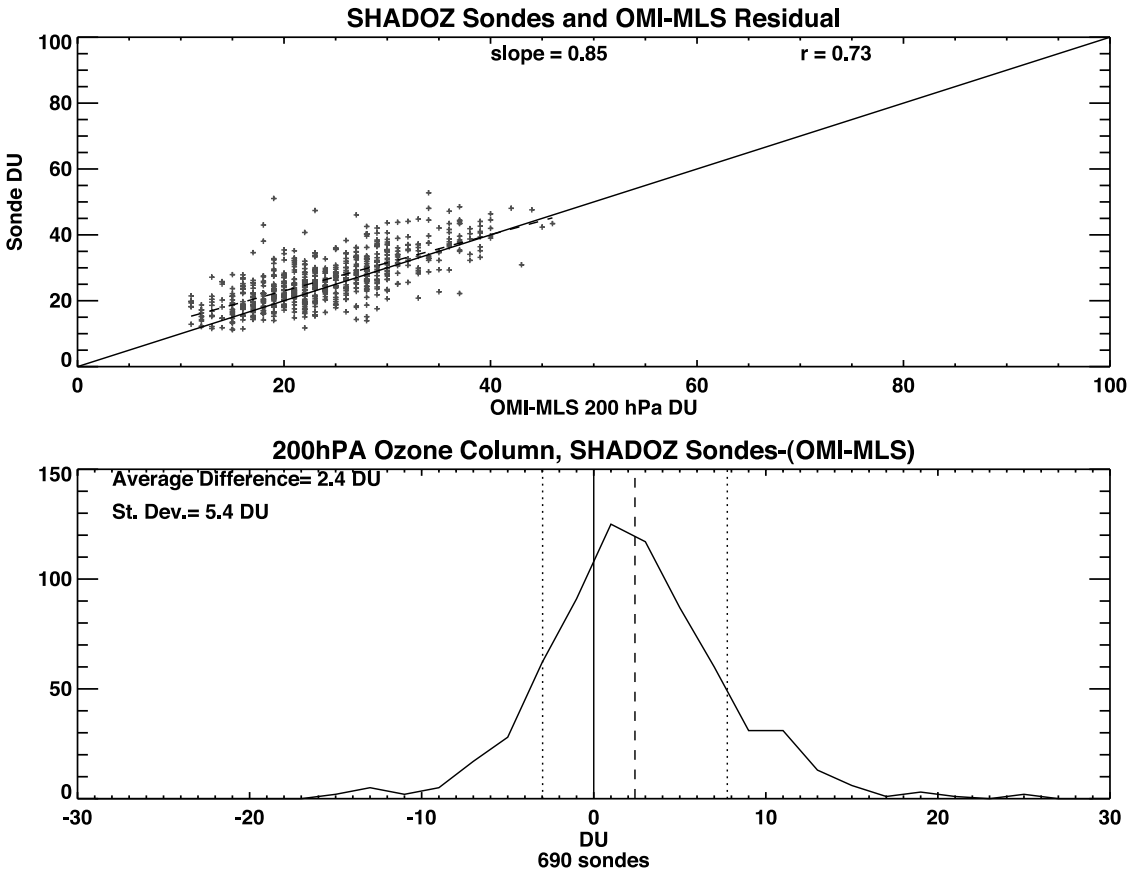


Figure 3. Comparison of ozonesondes 200TSC and our 200TSC estimate. (top) Data points, the slope of the data (dashed line) and the correlation coefficient (r). The one-to-one line is the solid line. (bottom) A PDF of the difference between the sonde 200TSC with the mean and standard deviation (dashed and dotted, respectively).

tropospheric column. They found poor agreement on a day-to-day basis but good agreement if the data were averaged into monthly means. A possible explanation for this is that the synoptic product generated by the simple subtraction of MLS stratospheric column from OMI total column ozone cannot account for the dynamic variation of the tropospheric column at extratropical latitudes. A monthly mean comparison would show better agreement since folds would average out. Our asynoptic TTOR does show a significant improvement over Z06 as is discussed below.

[22] As discussed above, we focus on the 200TSC to remove issues with the definition of the tropopause. This approach tests the concept of the residual technique itself and separates tropopause issues from the ozone data sets. For the comparison, ozone profiles from over 6,360 tropical and midlatitude ozonesondes have been used to compute the 200TSC. We use the Southern Hemisphere Additional Ozonesondes (SHADOZ) [*Thompson et al.*, 2003] collection, the European Space Agency Envisat Cal/Val collection, the WMO GAW collection and the IONS (INTEX Ozonesonde Network Study) collection [*Thompson et al.*, 2007]. The SHADOZ, GAW and Envisat sonde database covers late 2004 through 2006; IONS covers late February 2006 to September 2006. We compute the 200TSC using the OMI-MLS methods described above and bilinear interpolate the result (and the quality flags) to the sonde points; the sonde data have also been screened to within 6 h of the Aura overpass times.

3.1.1. SHADOZ Tropical Ozonesondes

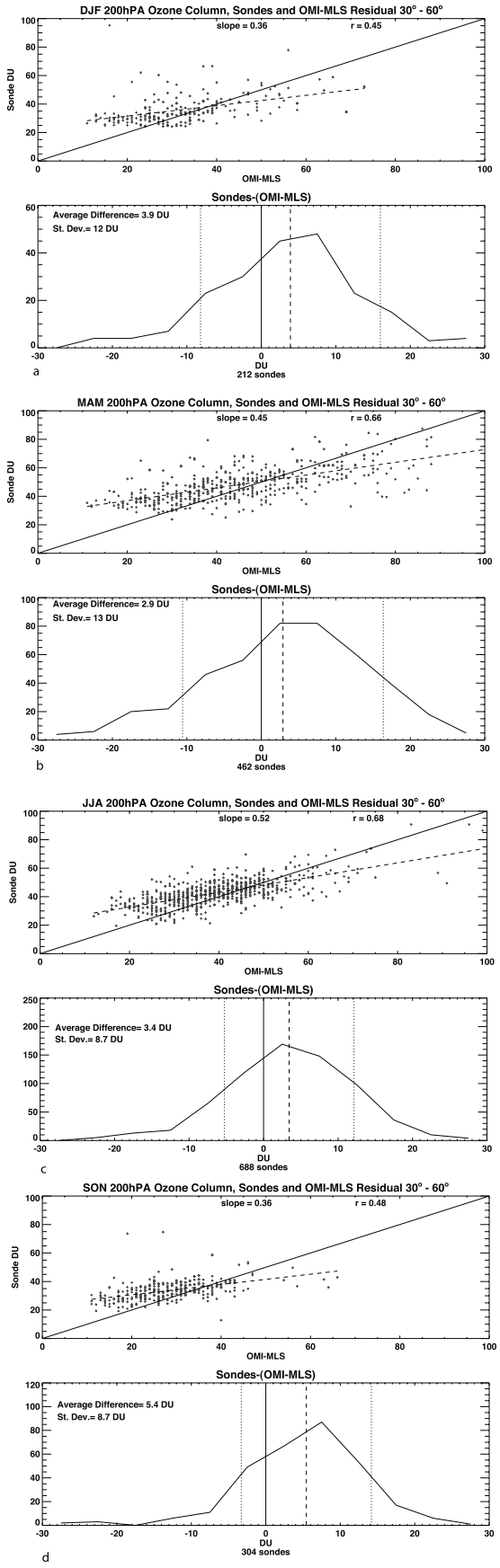
[23] In the midlatitudes, the tropospheric ozone amounts vary rapidly from day to day and from season to season. By comparison the tropical regions show relatively little rapid temporal variability. Thus there is no need to provide a seasonal analysis as done in the next section. SHADOZ data are used for our tropical comparisons.

[24] Figure 3 compares 690 ozonesonde estimates of the TTOR 200TSC over the Aura period. Estimates of instrumental errors are not included in the computation of the statistics. The comparison shows a correlation of 0.73 and a data slope of 0.85. The column offset is 2.4 DU with the ozonesonde profiles having a slightly higher column. This result would be consistent with a slightly high stratospheric column derived from MLS measurements. The standard deviation of $\sim$5 DU in this case represents the combined errors of the trajectory model, measurement error from both MLS and OMI as well as sonde error and thus probably represents the total uncertainty of the measurement.

3.1.2. Comparison With Midlatitude Ozonesondes by Season

[25] In Figure 4 we show the comparisons at midlatitudes by season. There are few ozonesondes in the extratropical

21562202d, 2007, D24, Downloaded from https://agupubs.onlinelibrary.wiley.com/doi/10.1029/2007JD008773 by Spanish Cochrane National Provision (Ministerio de Sanidad), Wiley Online Library on [22/01/2026]. See the Terms and Conditions (https://onlinelibrary.wiley.com/terms-and-conditions) on Wiley Online Library for rules of use; OA articles are governed by the applicable Creative Commons License



Southern Hemisphere so we restrict our analysis to the extratropical Northern Hemisphere.

[26] As was seen in the tropics, there is a persistent offset between our OMI-MLS 200TSC and the sonde 200TSC of about 3–5 DU depending on season. The correlation of the sonde and OMI-MLS data are weaker in fall and winter. The ozonesondes generally show less dynamic range than the residual product suggesting that the TTOR is influenced by lower stratospheric ozone since the tropopause is much lower in the middle latitudes. It is important to recognize that MLS vertical resolution is 2–3 km so that when there is a sharp ozone gradient at the tropopause, as occurs during winter, MLS may incorrectly estimate the stratospheric column. This would give the TTOR greater range than the ozonesonde column estimates.

[27] The *Froidevaux et al.* [2006] preliminary validation of MLS V1.5 ozone shows that MLS lower stratospheric ozone is slightly high biased to SAGE II and POAM. A 20% error in a typical midlatitude UTLS ozone profile would produce an stratospheric column increase of ~2–8 DU (depending on the profile) leading to a low bias in the TTOR of about the same amount as is seen above. J. Ziemke (personal communication, 2007) has compared OMI stratospheric column using cloud slicing with MLS stratospheric column and find that MLS is high biased by 2–3 DU consistent with our results.

[28] The figures also show that the TTOR-sonde difference standard deviation at midlatitudes is much larger than in the tropics. The greater fluctuation in the TTOR is due to greater fluctuations in the midlatitude stratospheric column. Nonetheless, although the midlatitude correlation with sonde data are not as good as in the tropics, the daily TTOR product does appear to provide information about the tropospheric ozone column.

[29] We have also correlated the TTOR with surface station ozone measurements and find only a very weak correlation of 0.12. It is not surprising that the TTOR is not very sensitive to surface values because OMI has low sensitivity to surface ozone due to strong Rayleigh scattering, and surface ozone variability tends to have a smaller spatial scale than the OMI pixel size (13x24 km at nadir) and thus is not well correlated.

3.2. Comparisons With Tropical TES Observations

[30] The Tropospheric Emission Spectrometer (TES) is an infrared Fourier transform spectrometer on Aura [*Beer*, 2006]. TES's high spectral resolution allows direct measurements of the tropospheric ozone. The TES ozone product and sonde validation are described by *Worden et al.* [2007] and G. B. Osterman et al. (Validation of Tropospheric Emission Spectrometer (TES) measurements of total column and stratospheric ozone, submitted to *Journal of Geophysical Research*, 2007, hereinafter referred to as Osterman et al., submitted manuscript, 2007). TES (like OMI) is not very sensitive to ozone at the surface because of lack of temperature contrast between the surface and the lowest atmospheric layer. Nonetheless, TES measurements

Figure 4. As in Figure 3, except midlatitude (30–60°N) sonde 200TSC and OMI-MLS 200TSC comparisons for four seasonal periods as indicated by the month grouping.

21562202d, 2007, D24, Downloaded from https://agupubs.onlinelibrary.wiley.com/doi/10.1029/2007JD008773 by Spanish Cochrane National Provision (Ministerio de Sanidad), Wiley Online Library on [22/01/2026]. See the Terms and Conditions (https://onlinelibrary.wiley.com/terms-and-conditions) on Wiley Online Library for rules of use; OA articles are governed by the applicable Creative Commons License

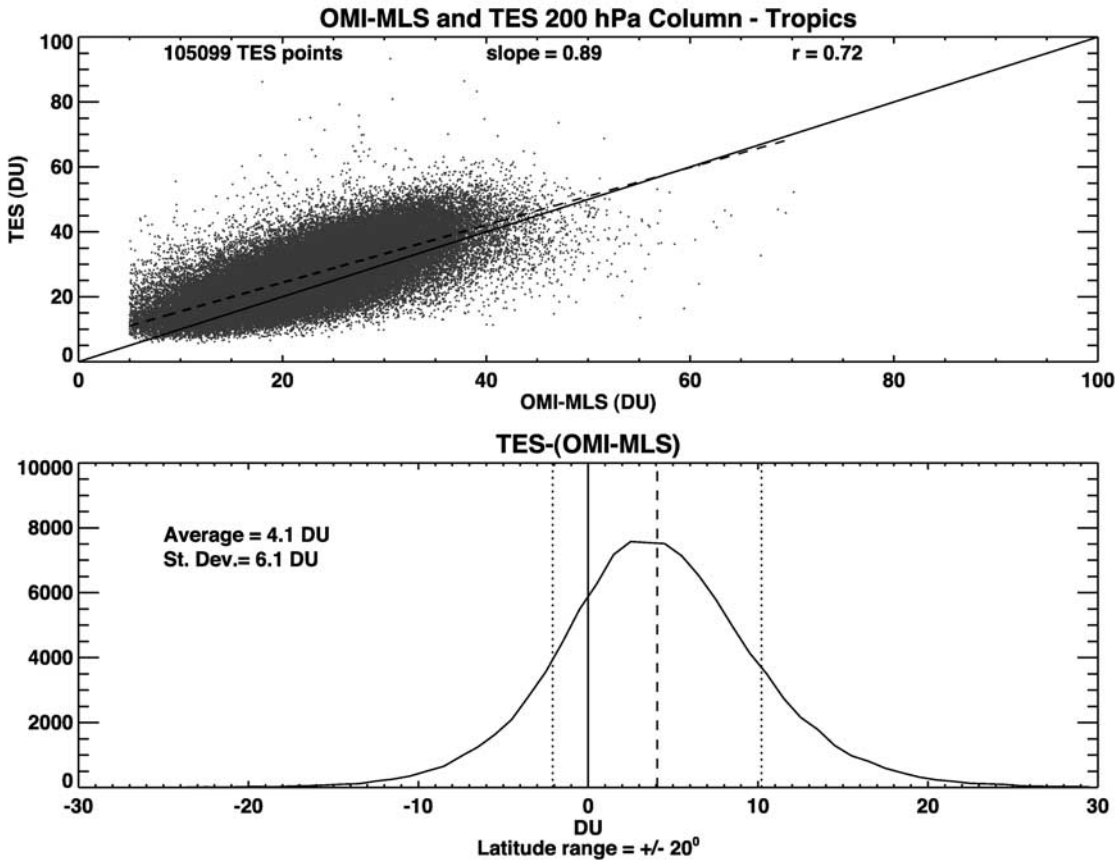


Figure 5. As with Figure 3 except comparisons with TES measurements.

should provide a reasonable estimate of the tropospheric column for comparison. As with the sonde comparison we compute the TES 200TSC and interpolate our 200TSC to the TES locations. We use TES data taken from 1 October 2004 through 20 September 2006. TES tropospheric columns were created by integrating the TES reported profile up to 200 hPa. The error for the column can be calculated using the reported profile error covariance, as discussed by *Kulawik et al.* [2006]. Figure 5 shows the comparison with TES tropical data using ~100,000 points. Comparisons are not screened to local daylight so this group also includes TES measurements at night; in the tropics where ozone varies slowly, the day-night distinction is probably unimportant. Values are cut off at 5 DU for both data sets; it is unlikely that tropospheric column values can ever be that low.

[31] In the tropical regions, the TES and TTOR are in good agreement and correlate well. We note a high bias of about 4.1 DU for TES with a standard deviation of 6.1 DU. Osterman et al. (submitted manuscript, 2007) found TES high biased by about 3.6 DU compared to near coincident ozonesondes on a global average with a standard deviation of 6.8 DU. *Kulawik et al.* [2006] found that TES total ozone column was high biased with respect to OMI column (see their Figure 8, ~12.5 DU). Our results are generally consistent with Osterman et al.'s (submitted manuscript, 2007) and *Kulawik et al.*'s [2006] findings. The Gaussian structure of the difference PDF suggests that the differences between TTOR are due to random error.

3.3. Seasonal Extratropical Comparisons With the TES Data

[32] Figure 6 shows the comparison of the extratropical data (30–50°N). The correlation between the data sets is not as high in the extratropics (0.43–0.54) as we saw in the tropics (0.6). The biases vary between 0.8 and 7 DU with larger standard deviations than in the tropics. As with our sonde comparison, TES dynamical range is smaller than the TTOR.

3.4. Summary of Validation Results

[33] Table 1 summarizes the bias and standard deviations for both the ozonesondes and TES. There is very good agreement in the tropics between the TTOR and the ozonesonde and TES data sets. Outside the tropics there is a wider range in the TTOR 200TSC than seen in TES or sonde 200TSC. The best extratropical agreement is in summer when the extratropical tropopause is highest, in other words, when extratropical tropopause is elevated like the tropical tropopause. These results suggest that the TTOR is less reliable under low tropopause conditions, when ozone levels are high in the 100–200 hPa UTLS region.

[34] There is a persistent offset between the TTOR and TES or ozonesondes. The TTOR is low biased which could arise either from a high bias in the MLS stratospheric

21562202d, 2007, D24, Downloaded from https://agupubs.onlinelibrary.wiley.com/doi/10.1029/2007JD008773 by Spanish Cochrane National Provision (Ministerio de Sanidad), Wiley Online Library on [22/01/2026]. See the Terms and Conditions (https://onlinelibrary.wiley.com/terms-and-conditions) on Wiley Online Library for rules of use; OA articles are governed by the applicable Creative Commons License

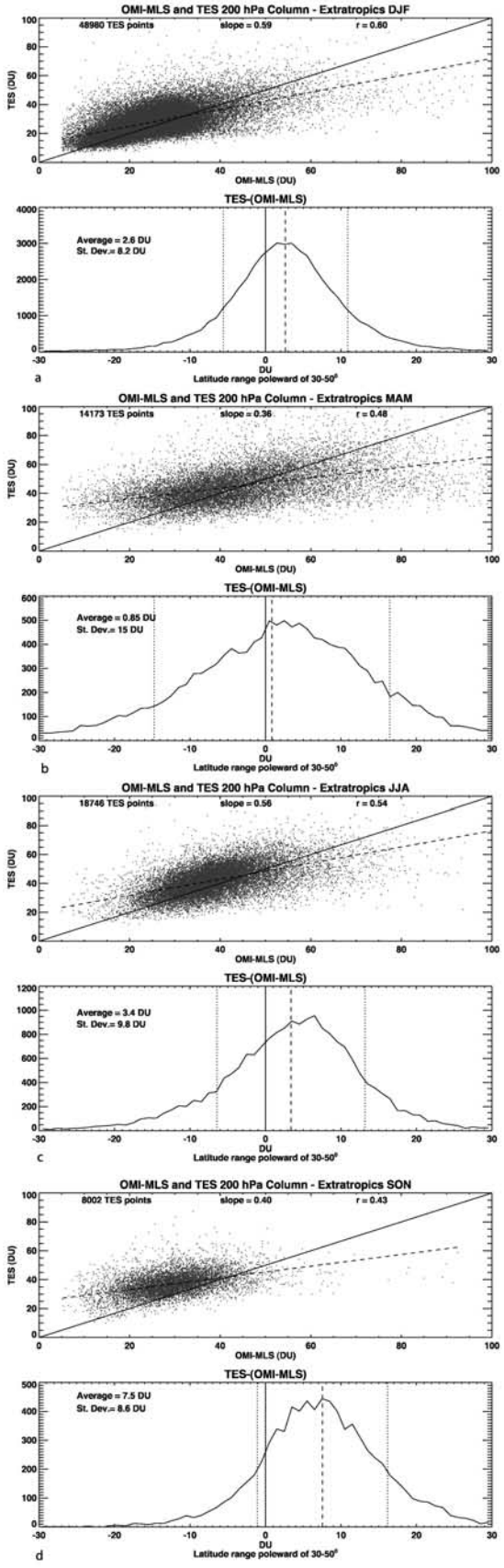


Figure 6. Same as Figure 4 except comparing TES 200 hPa extratropical column (30–50°N) with OMI-MLS 200 hPa column.

column or a low bias with the OMI ozone column. McPeters et al.'s (submitted manuscript, 2007) comparison of OMI column ozone with ground stations shows no persistent bias suggesting that the problem lies with the MLS stratospheric column. J. Ziemke (personal communication, 2007) has found that the OMI stratospheric column obtained by cloud slicing is consistently lower than the MLS stratospheric column by several DU. *Froidevaux et al.* [2006] also show a high bias in the 100–200 hPa region which could create an stratospheric column bias.

[35] Is this product an improvement over the Z06 daily product? In Table 2 we show comparisons of Z06 with the sonde data to determine whether this approach produces an improved product. In comparison with Table 1 we can see that the standard deviation, biases are lower and correlation coefficients are higher with this product than with Z06 for each season and region. We can conclude that the daily TTOR product is an improvement over Z06.

4. Daily and Monthly Maps of Tropospheric Average Mixing Ratio

4.1. Daily Values

[36] As mentioned above the midlatitude tropospheric ozone residual values are strongly affected by high levels of ozone in the UTLS as occurs with stratosphere-troposphere exchange (STE) processes. This is illustrated in Figure 7 which shows the tropospheric average mixing ratio for a sequence of 4 d from 20 to 23 May 2006.

[37] Figure 7 shows that the strong gradients in the tropopause are frequently colocated with the tropospheric average mixing ratio maxima suggesting that the residual is strongly influenced by upper tropospheric folding processes [e.g., *de Laat et al.*, 2005, and references therein]. For example, the mid-Pacific maximum on 21 May are clearly due to a folding event. Simultaneously, a folding event is occurring off the east coast of the United States.

4.2. Annual Mean Values

[38] Folds are highly mobile events and tend to average out of monthly and annual mean data. Figure 8 shows the column residual and tropospheric average mixing ratio for 2005 and 2006.

[39] Values are reported on this map if 10 d of high-quality data can be used for a pixel. Both maps show the characteristics described by Z06 including high values of the eastern U. S., high values covering Europe, especially

Table 1. Summary of 200TSC Validation Results[a]

		NH Extratropics			
Comparison	Tropics	DJF	MAM	JJA	SON
Ozonesonde					
Biases, DU	2.4	3.9	2.9	3.4	5.4
Standard deviation	5.4	12	13	8.7	8.7
Correlation coefficient	0.73	0.45	0.66	0.68	0.48
TES					
Biases	4.1	2.6	0.85	3.4	7.5
Standard deviation	6.1	8.2	15	9.8	8.6
Correlation coefficient	0.72	0.6	0.48	0.54	0.43

[a]Biases are positive when OMI-MLS is low compared to the other data set.

21562202d, 2007, D24, Downloaded from https://agupubs.onlinelibrary.wiley.com/doi/10.1029/2007JD008773 by Spanish Cochrane National Provision (Ministerio de Sanidad), Wiley Online Library on [22/01/2026]. See the Terms and Conditions (https://onlinelibrary.wiley.com/terms-and-conditions) on Wiley Online Library for rules of use; OA articles are governed by the applicable Creative Commons License

Table 2. Z06 Versus Sonde Comparison

		NH Extratropics			
Z06 200-hPa-Surface Ozone	Tropics	DJF	MAM	JJA	SON
Ozonesonde					
Biases, DU	5.2	4.5	8.8	8.5	7.1
Standard deviation	6.1	18	17	13	10
Correlation coefficient	0.622	0.36	0.4	0.37	0.19

the Mediterranean [*Lelieveld et al.*, 2002] to east Asia extending into the Pacific to the West Coast of the U.S. We also note the very low values over the tropical east Pacific region [*Kley et al.*, 1996; *Martin et al.*, 2002]. Note the decrease in DU values in the presence of high topography near continental edges or in mountain ranges (Figure 8, top). This decrease is not present in the mixing ratio plots (Figure 8, bottom). The decrease is due the change in surface pressure where the topography is high so the total column is smaller (see equation (1)). This pressure column effect has less impact on the average mixing ratio.

[40] Aside from the similarity between years, there is visible interannual variability. For example, the high ozone features in the South Atlantic and Africa [see, e.g., *Edwards et al.*, 2003; *Moxim and Levy*, 2000; *Marufu et al.*, 2000; *Thompson et al.*, 1996; *Fishman and Larsen*, 1987] are more extensive in 2005 than in 2006. Monthly mean data are not shown here but can be downloaded ftp://hyperion.gsfc.nasa.gov/pub/aura/tropo3/tropo3_YYMM.pdf where MM indicates the month number (e.g., 06) and YY the year number (e.g., 05). The data range from October 2004 through 2006, "0410" to "0612."

[41] Figure 9 shows the zonal mean tropospheric ozone residual verses time for three cases, globally, the Atlantic sector (75°W–15°E) and the Pacific sector (135°E–120°W). Once each month OMI performs a zoom in maneuver which leaves a gap in the global data due to incomplete swaths. Between ±60° the data shown in Figure 9 is interpolated across the gaps.

[42] Figure 9 shows that the increase in the residual in the Northern Hemisphere (NH) begins in April starting at ~20°N and moving northward. Ozone begins to decrease in August and minimizes during winter. In the Southern Hemisphere (SH), a similar increase develops in September at 20°S and at 60°S. In the tropics, the zonal mean minimum occurs from late January to June.

[43] The midlatitude spring NH increase likely begins with influx of ozone from the stratosphere that occurs in late winter. The build up continues through July with increases in tropospheric ozone due to pollution. In the SH a similar increase occurs at 30–40°S. This increase is enhanced by

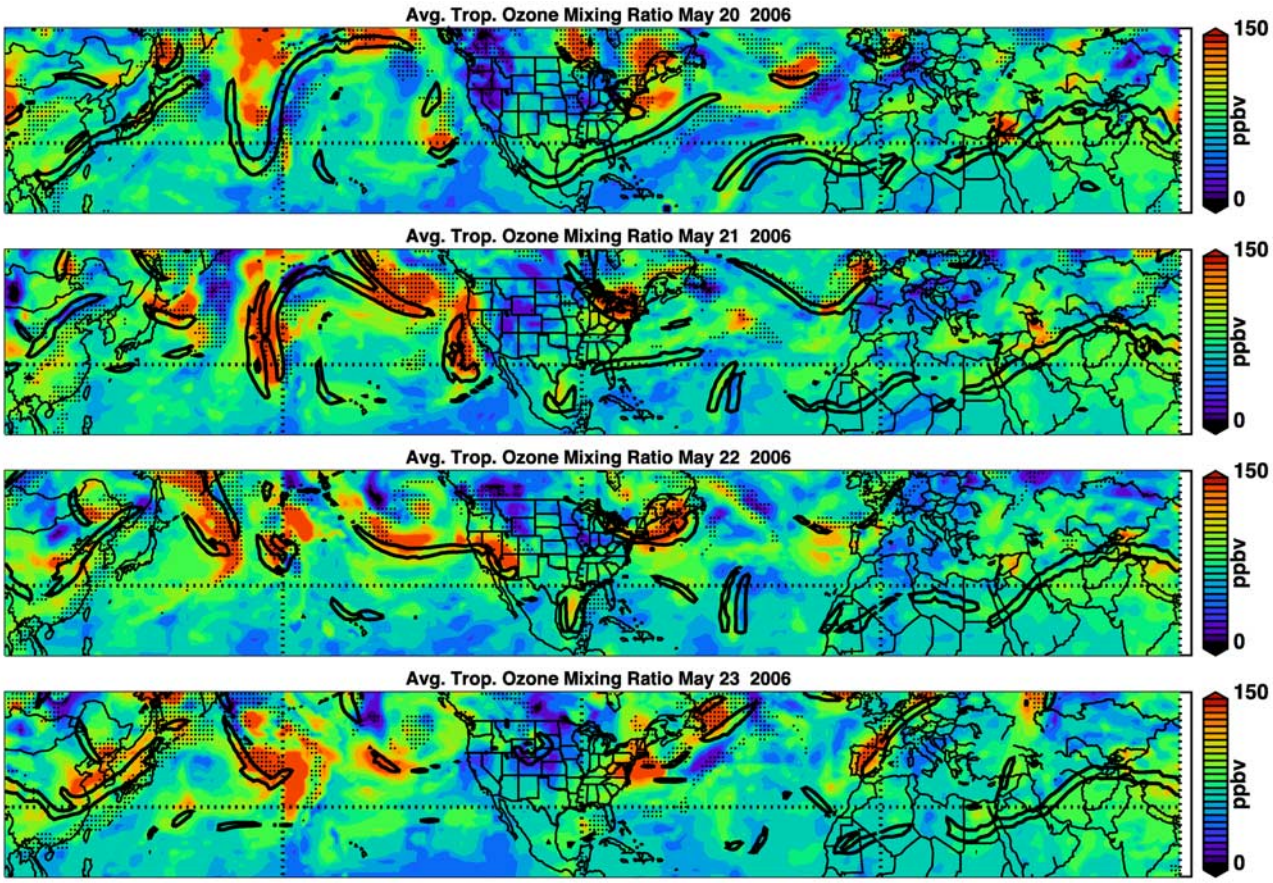


Figure 7. Tropospheric averaged mixing ratio for the sequence 20–23 May 2006. Black contours surround regions where there is a maximum in the tropopause spatial gradient, an indicator of fold locations. Small black dots indicate regions where the data are of questionable quality (i.e., high reflectivity, low tropopause, etc.)

21562202d, 2007, D24, Downloaded from https://agupubs.onlinelibrary.wiley.com/doi/10.1029/2007JD008773 by Spanish Cochrane National Provision (Ministerio de Sanidad), Wiley Online Library on [22/01/2026]. See the Terms and Conditions (https://onlinelibrary.wiley.com/terms-and-conditions) on Wiley Online Library for rules of use; OA articles are governed by the applicable Creative Commons License

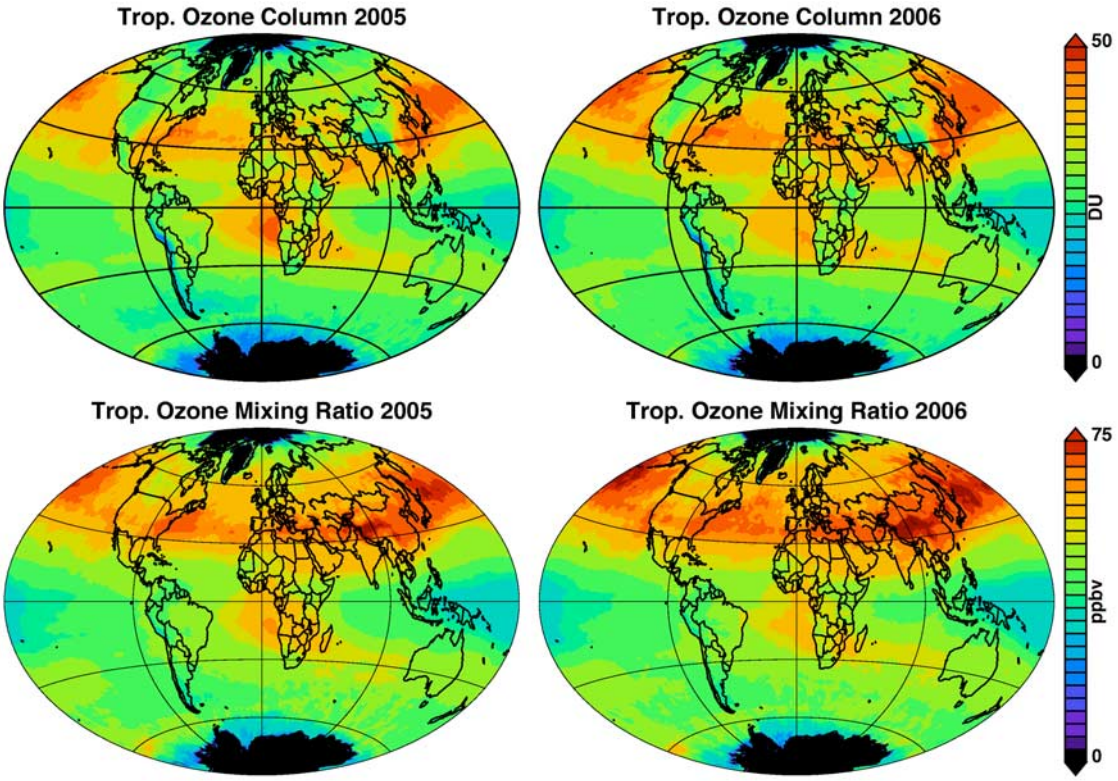


Figure 8. Annual mean maps of TTOR and tropospheric average mixing ratio for 2005 and 2006.

21562202d, 2007, D24, Downloaded from https://agupubs.onlinelibrary.wiley.com/doi/10.1029/2007JD008773 by Spanish Cochrane National Provision (Ministerio de Sanidad), Wiley Online Library on [22/01/2026]. See the Terms and Conditions (https://onlinelibrary.wiley.com/terms-and-conditions) on Wiley Online Library for rules of use; OA articles are governed by the applicable Creative Commons License

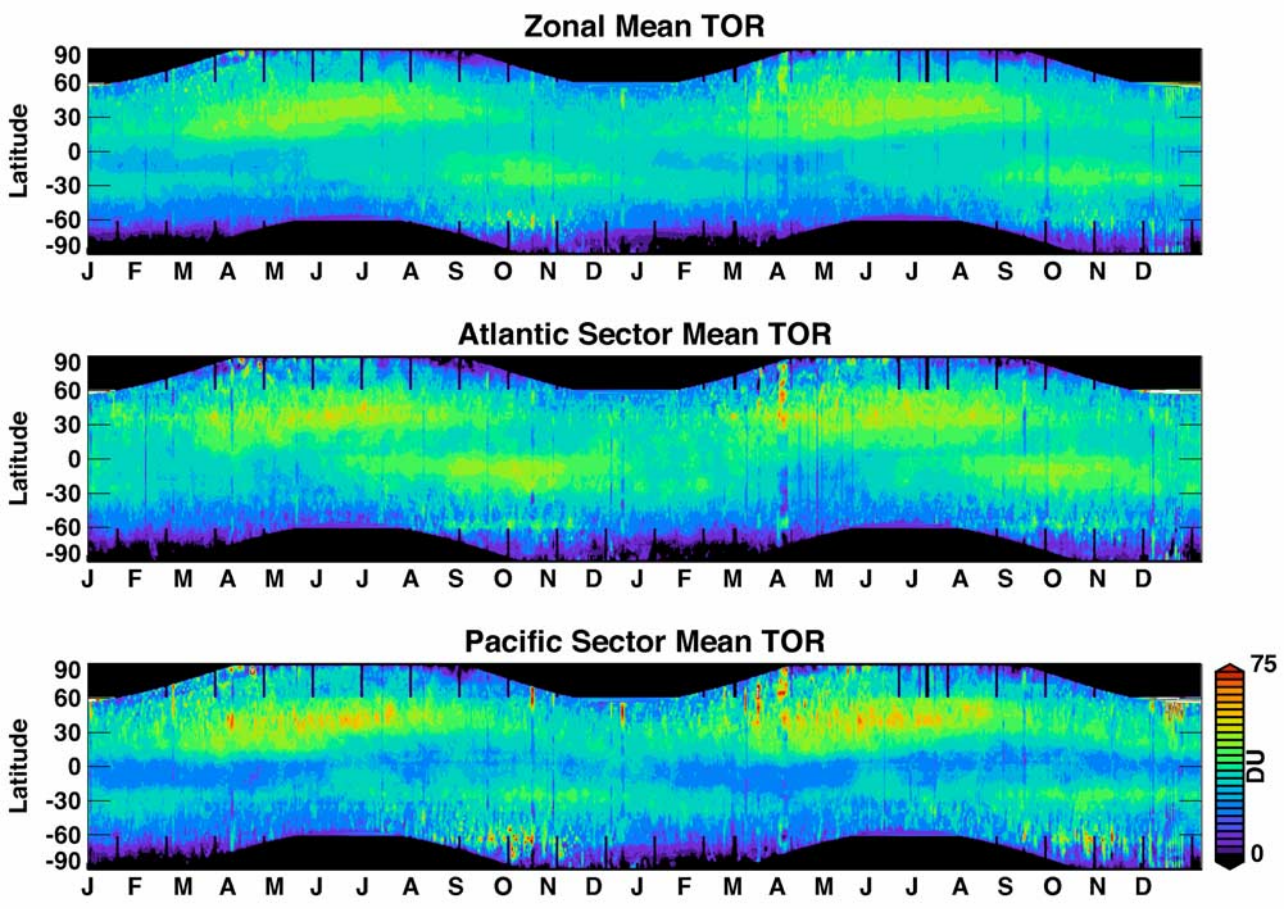


Figure 9. (top) Zonal mean tropospheric ozone for 2005–2006. (middle) Atlantic sector mean ozone 75°W–15°E. (bottom) Pacific sector mean ozone 135°E–120°W.

21562202d, 2007, D24, Downloaded from https://agupubs.onlinelibrary.wiley.com/doi/10.1029/2007JD008773 by Spanish Cochrane National Provision (Ministerio de Sanidad), Wiley Online Library on [22/01/2026]. See the Terms and Conditions (https://onlinelibrary.wiley.com/terms-and-conditions) on Wiley Online Library for rules of use; OA articles are governed by the applicable Creative Commons License

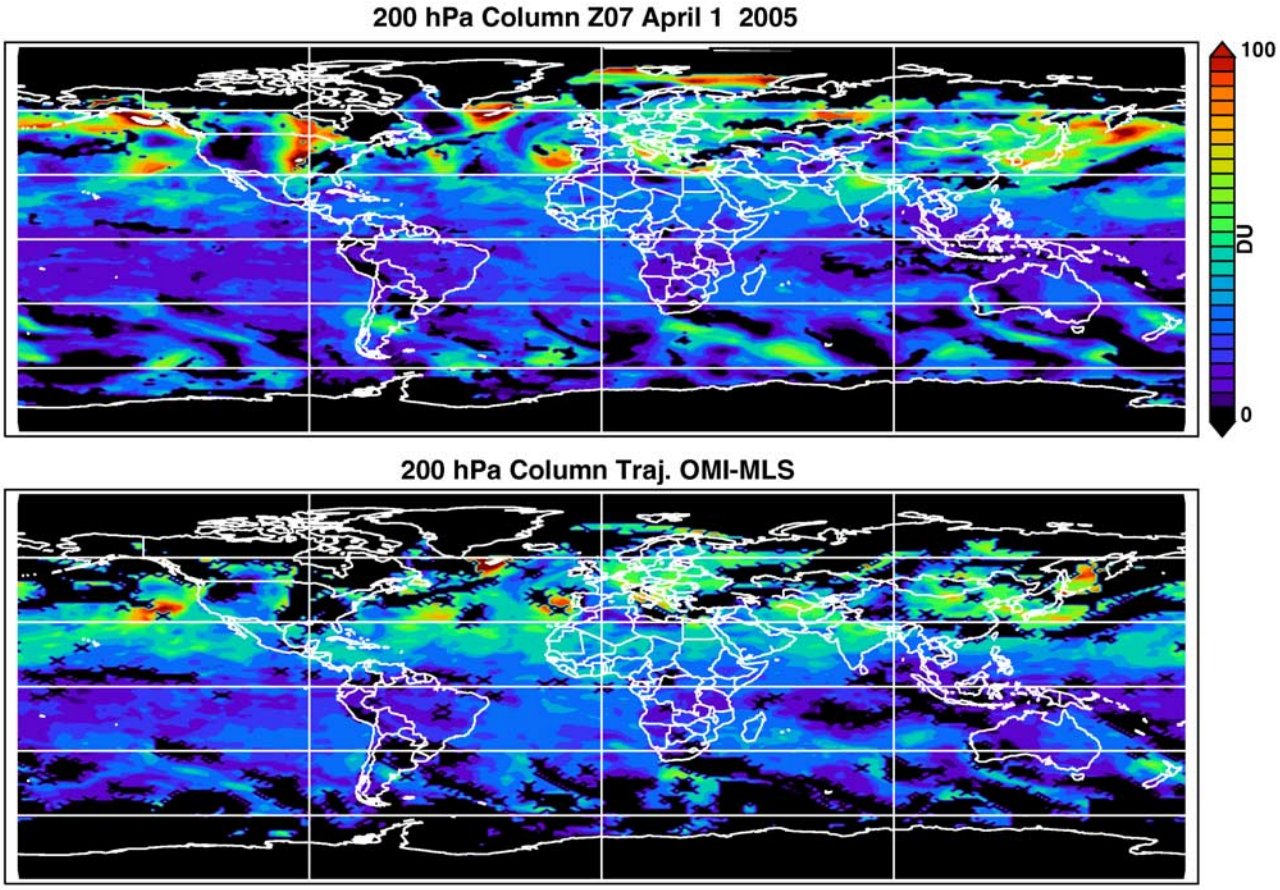


Figure 10. (top) The 200TSC for 1 April 2005 calculated using the algorithm in Z06. (bottom) TTOR 200TSC interpolated to the Z06 grid. Dark areas are flagged regions meaning the results are questionable because of, for example, high reflectivity or low tropopause.

African and South American biomass burning which gives rise to the South Atlantic anomaly [e.g., *Edwards et al.*, 2003; *Thompson et al.*, 1996; *Fishman and Larsen*, 1987] also seen in the annual mean (Figure 8). The biomass burning enhancement shows up clearly in the contrast between the Atlantic and Pacific sectors seen in Figure 9. In the tropics, very low ozone occurs in the Pacific sector as a result of convection and tropopause uplift.

5. Comparison to Z06

[44] The Z06 method and TTOR produce different results as was shown in the sonde comparisons given in Table 2. Figure 10 shows 1 April 2005 for Z06 and the TTOR interpolated to the Z06 grid. Black regions in both maps indicate where the data has been flagged for quality. Generally the maps are similar except for the very high and low regions in Z06, most of which have been flagged in the TTOR lower figure (e.g., the high TOR patch over mid-North America). The very low tropospheric ozone residual region in western North America is significantly lower in Z06 than with TTOR. We have been able to show that very high and low TTOR regions (that are often paired, such as in this example) are the of result of assuming that the MLS and OMI data are synoptic; that is, the MLS and OMI data do not need to be synchronized to the same local time. However, when the local times are used these anomalies tend to be greatly reduced, as in this example. The reduction occurs because events like the one shown in the picture move rapidly even in a single day and the small offset between the stratospheric column and the total column generated by lack of time synchronization can produce aliasing in the residual.

[45] Figure 11 shows a tropical comparison of Z06 and TTOR. We don't expect a perfect correlation because of the different scheme for creating the high-resolution stratosphere, nonetheless, the correlation is quite high. The offset of 2.3 DU is due to ozone explicitly added to the Z06 product based on recent evaluation of OMI and MLS stratospheric column offset differences for September 2004 to December 2006 (J. Ziemke, personal communication, 2007). The difference PDF is Gaussian with a fairly small standard deviation, ~4 DU, reflecting the overall similarity between the schemes.

[46] Figure 12 shows the midlatitude comparison for July 2005. The correlation coefficient is high despite the higher scatter. We also see an offset of about 6.5 DU which is not entirely due to the explicit addition of ozone in Z06. Referring back to Figure 10 (which shows 1 d) we see that there are higher values in the Z06 product compared to this one because of the synoptic assumptions in that calculation. This creates a skewed distribution and a higher mean bias

21562202d, 2007, D24, Downloaded from https://agupubs.onlinelibrary.wiley.com/doi/10.1029/2007JD008773 by Spanish Cochrane National Provision (Ministerio de Sanidad), Wiley Online Library on [22/01/2026]. See the Terms and Conditions (https://onlinelibrary.wiley.com/terms-and-conditions) on Wiley Online Library for rules of use; OA articles are governed by the applicable Creative Commons License

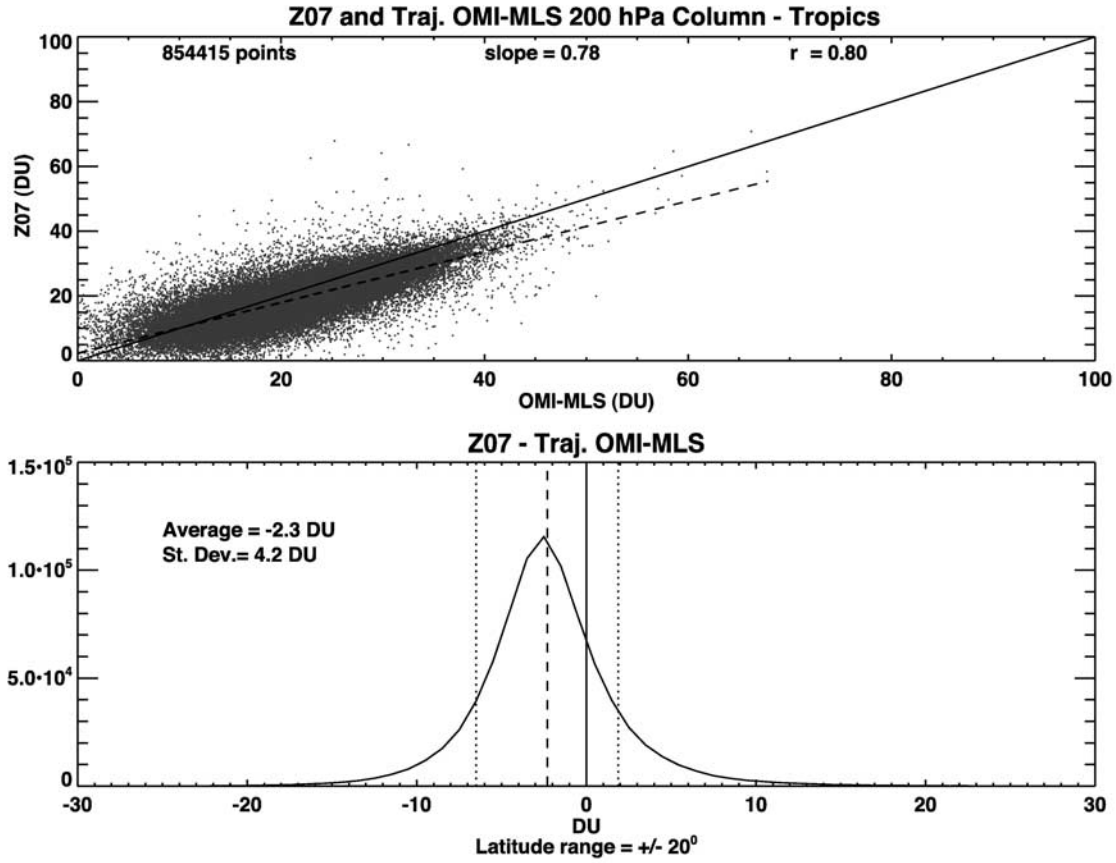


Figure 11. Comparison of this OMI-MLS 200 hPa column to surface product with Z06 in the region ±20° latitude as in Figure 3.

21562202d, 2007, D24, Downloaded from https://agupubs.onlinelibrary.wiley.com/doi/10.1029/2007JD008773 by Spanish Cochrane National Provision (Ministerio de Sanidad), Wiley Online Library on [22/01/2026]. See the Terms and Conditions (https://onlinelibrary.wiley.com/terms-and-conditions) on Wiley Online Library for rules of use; OA articles are governed by the applicable Creative Commons License

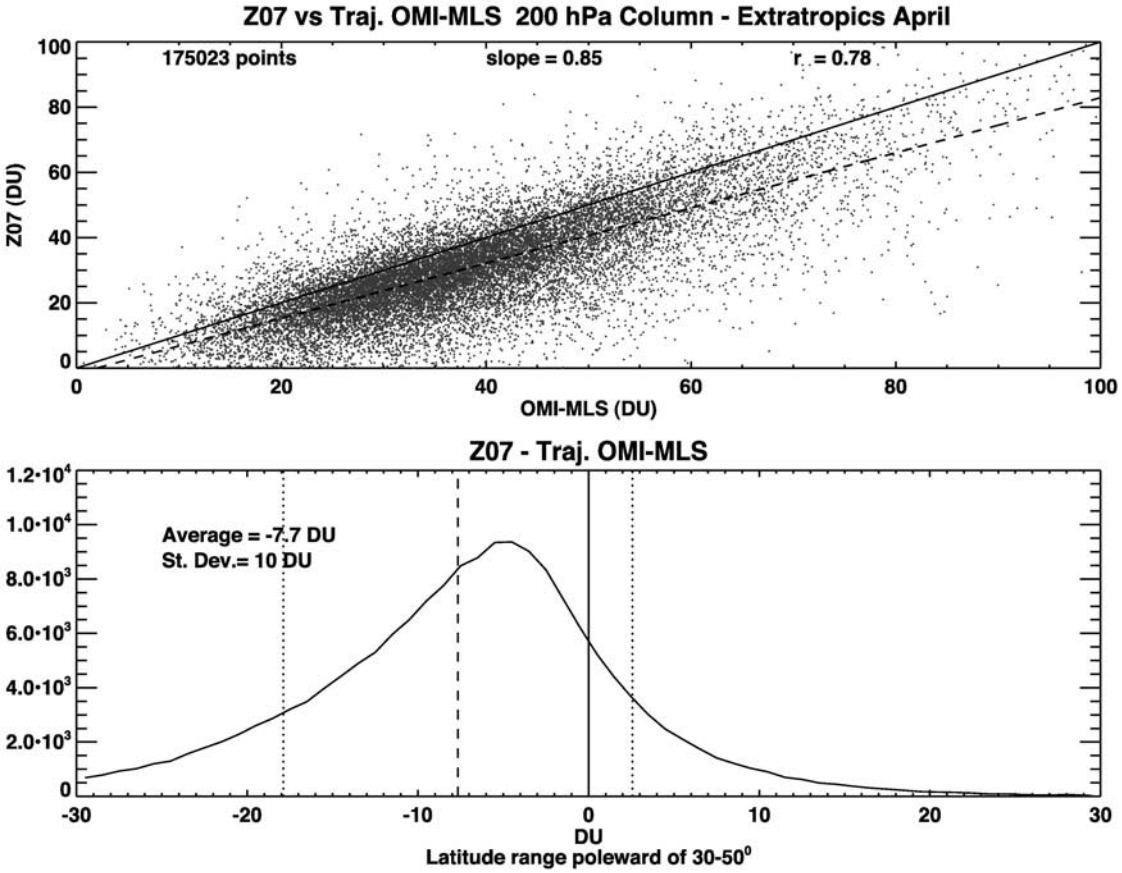


Figure 12. Comparison of the 200TSC from Z06 and this product for April 2005 as in Figure 11. Extratropical range is 30°N to 50°N latitude.

21562202d, 2007, D24, Downloaded from https://agupubs.onlinelibrary.wiley.com/doi/10.1029/2007JD008773 by Spanish Cochrane National Provision (Ministerio de Sanidad), Wiley Online Library on [22/01/2026]. See the Terms and Conditions (https://onlinelibrary.wiley.com/terms-and-conditions) on Wiley Online Library for rules of use; OA articles are governed by the applicable Creative Commons License

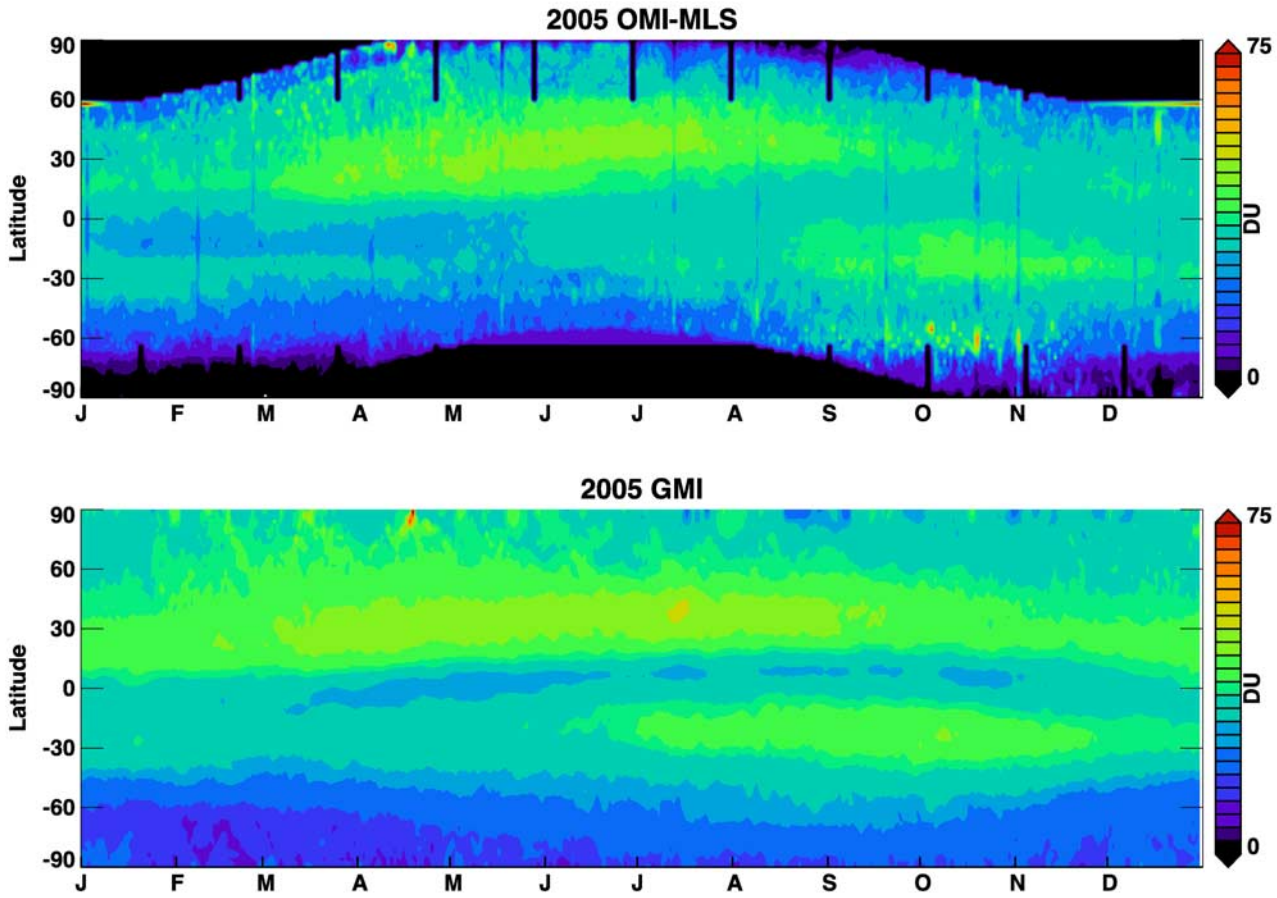


Figure 13. Zonal mean annual cycle for 2005 with this product and the zonal mean GMI ozone residual shown in Figure 9.

shown in Figure 12. Other months (not plotted here) show similar results.

6. Comparison With the Global Modeling Initiative Combined Stratosphere-Troposphere CTM

[47] Z06 describe the Global Modeling Initiative (GMI) chemical transport model. The GMI model includes both tropospheric and stratospheric chemistry. This model has been recently rerun, updating the chemistry and pollution sources. The results are shown in Figure 13 and are compared the TTOR zonal mean results from Figure 9. Overall the GMI model agrees with the TTOR estimates; however, we note some important differences. TTOR values at high zenith angles appear to be systematically lower than GMI. The GMI model also shows slightly lower tropical tropospheric values from June through November, and slightly higher tropical values from January-March. We also see a wider band of high ozone values at subtropical latitudes in GMI than in the TTOR.

[48] Figure 14 shows a single day comparison between the GMI model and the TTOR product. Overall the GMI and the TTOR products are quite close, even some extreme features such as the high ozone field off the tip of Greenland are represented. However, there are some differences that warrant further investigation such as the high feature between Hawaii and the west coast of the United States that appears to be only weakly represented in the GMI product. We also note lower ozone amounts over South America and equatorial Africa. Figure 15 shows the difference statistics between the tropical GMI and the TTOR 200TSC for April 2005. There is a good correlation and the offset is about 2 DU; the standard deviation is about 5 DU and the statistics are Gaussian suggesting that the differences are fairly random.

[49] Midlatitude comparison with GMI shows poorer agreement as seen in Figure 16. There is poorer correlation and a wider distribution of differences. Overall, the GMI column variation has a much smaller ozone column range. This smaller range is also evident in the single day comparison shown in Figure 14.

7. Summary

[50] Forward trajectories are used to increase the spatial resolution of the stratospheric ozone column in order to produce a higher-resolution tropospheric column ozone using the residual method. We use the OMI-Total Ozone Mapping Spectrometer algorithm for the total column and MLS V1.5 for the stratosphere. We refer to this product as the Trajectory Total Ozone Residual (TTOR). We compare

21562202d, 2007, D24, Downloaded from https://agupubs.onlinelibrary.wiley.com/doi/10.1029/2007JD008773 by Spanish Cochrane National Provision (Ministerio de Sanidad), Wiley Online Library on [22/01/2026]. See the Terms and Conditions (https://onlinelibrary.wiley.com/terms-and-conditions) on Wiley Online Library for rules of use; OA articles are governed by the applicable Creative Commons License

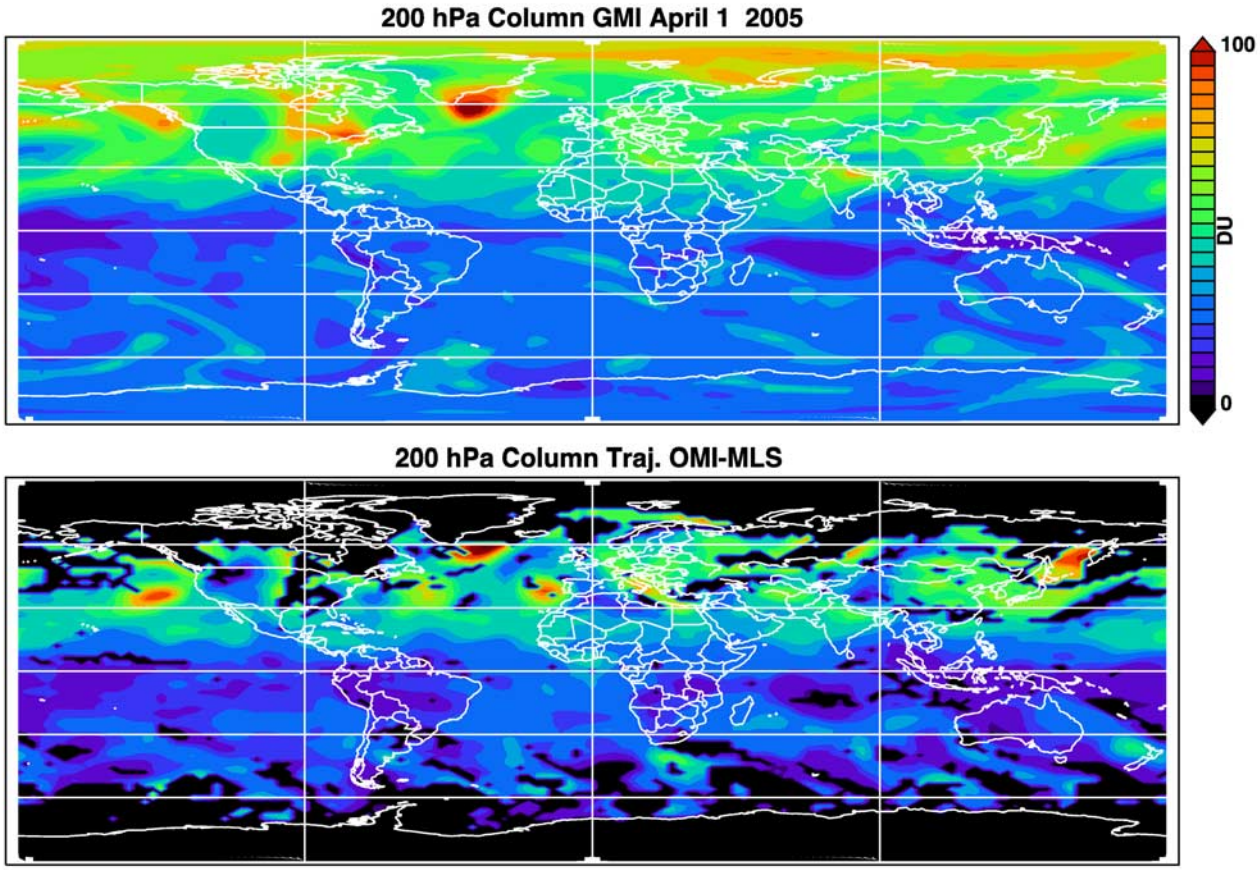


Figure 14. (top) The 1 April 2005 GMI and (bottom) the TTOR 200TSC.

21562202d, 2007, D24, Downloaded from https://agupubs.onlinelibrary.wiley.com/doi/10.1029/2007JD008773 by Spanish Cochrane National Provision (Ministerio de Sanidad), Wiley Online Library on [22/01/2026]. See the Terms and Conditions (https://onlinelibrary.wiley.com/terms-and-conditions) on Wiley Online Library for rules of use; OA articles are governed by the applicable Creative Commons License

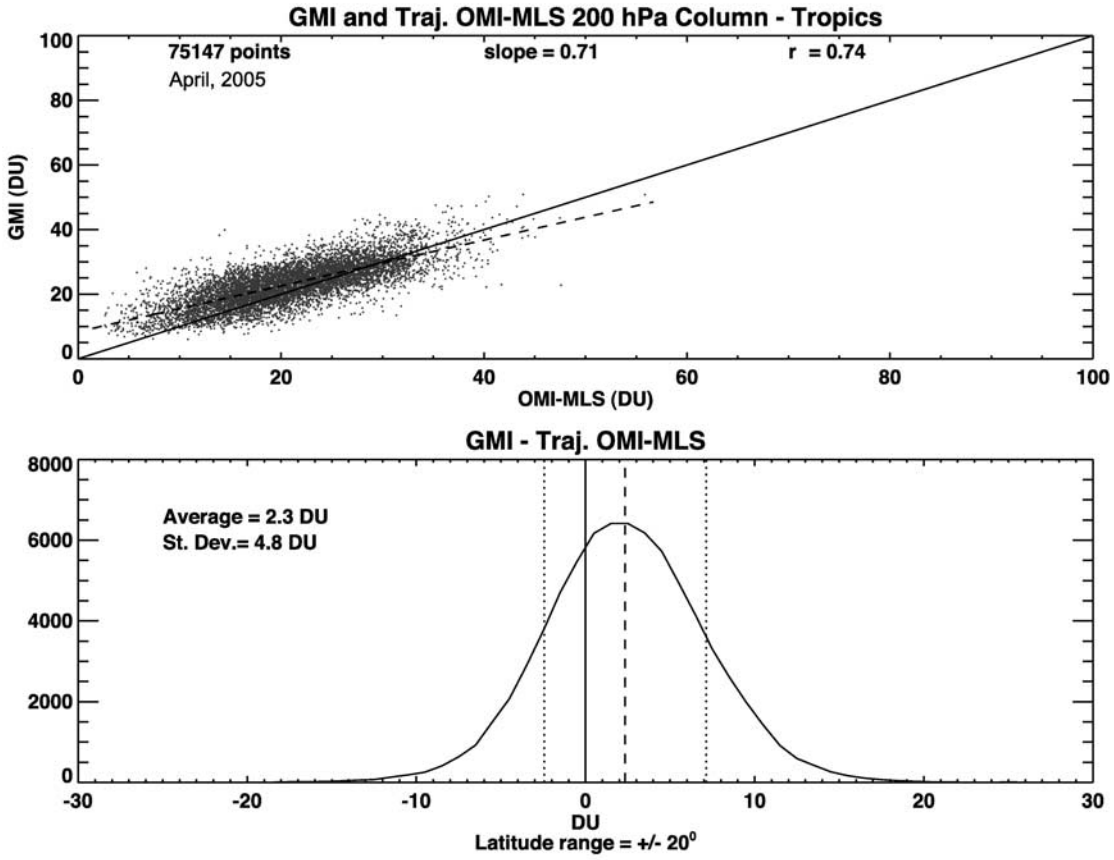


Figure 15. Comparison of the TTOR and GMI 200TSC in the region ±20° latitude as in Figure 3.

21562202d, 2007, D24, Downloaded from https://agupubs.onlinelibrary.wiley.com/doi/10.1029/2007JD008773 by Spanish Cochrane National Provision (Ministerio de Sanidad), Wiley Online Library on [22/01/2026]. See the Terms and Conditions (https://onlinelibrary.wiley.com/terms-and-conditions) on Wiley Online Library for rules of use; OA articles are governed by the applicable Creative Commons License

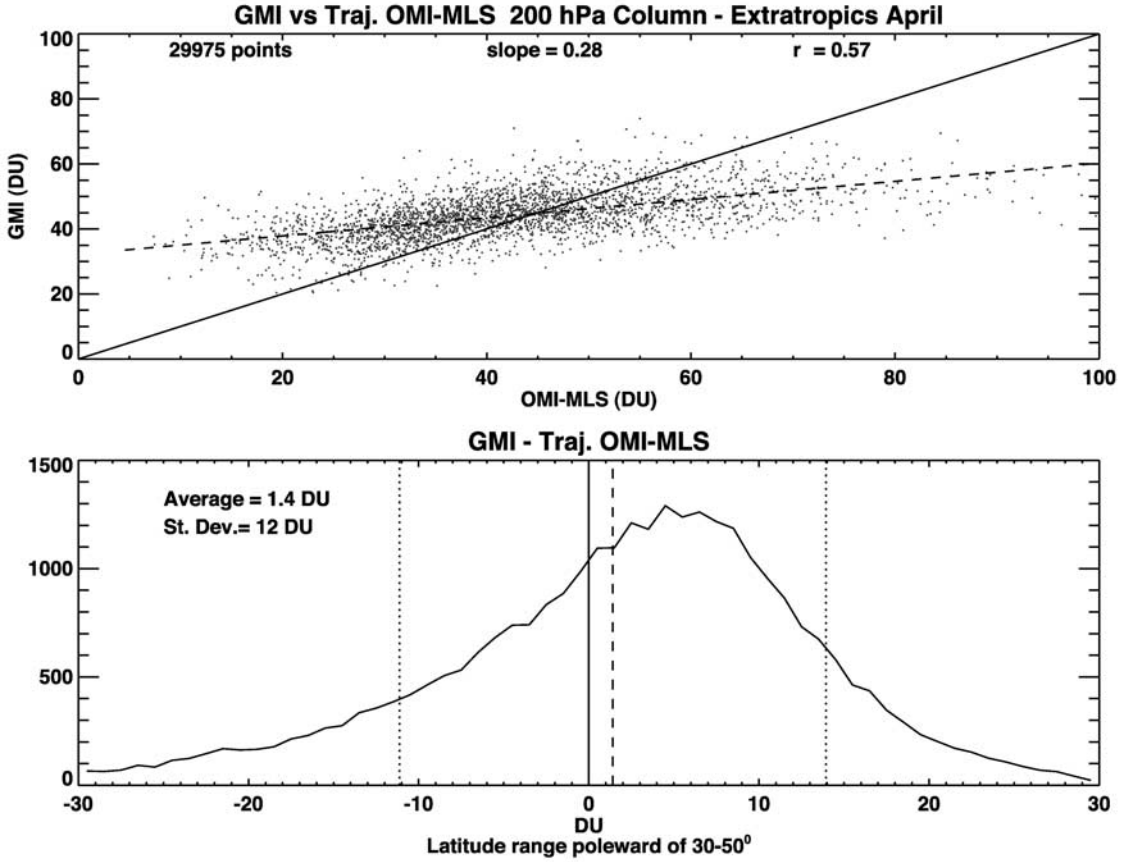


Figure 16. Northern midlatitude comparison of GMI and the OMI-MLS surface to 200 hPa product.

the 200-hPa-to-surface column (200TSC) TTOR against the 200TSC from sondes and TES measurements. Using the 200TSC removes issues associated with different tropopause definitions. Comparisons with sondes and TES show good agreement in the tropics and reasonable agreement at middle latitudes. TTOR is an improvement over the Z06 daily product as is shown by comparison to sondes. Nonetheless there is a persistent low bias in the TTOR which appears to be due to high bias in the MLS (V1.5) lower stratospheric mixing ratio. This low bias led Z06 to add 2.3 DU of ozone to their product which shows up in our comparisons with their product. We also note that there is much more variability in the midlatitude TTOR than ozonesondes show. This is probably due to the fact that MLS, with its 3–4 km weighting function and lower precision in the lower stratosphere, cannot resolve the steep ozone gradient at the midlatitude tropopause.

[51] There is a strong correlation of extratropical tropospheric column anomalies with probable troposphere-stratosphere folds that are identified by large tropopause height gradients. Tropospheric ozone residual anomalies due to folds may be mistaken for pollution events since they often occur in the Atlantic and Pacific pollution corridors. We also compare the 200TSC with GMI estimates of the tropospheric column. While the tropical comparisons are good, we note that GMI variations in 200TSC at middle latitudes are much smaller than those estimated using TTOR thus GMI is somewhat closer to the ozonesondes analysis; however, more extensive comparisons between GMI and ozonesondes remain to be done.

[52] **Acknowledgments.** Ozonesonde data were obtained through the NASA Aura Validation Data Center and contributions from the ESA Envisat Cal/Val data center and the WMO GAW regional collection center for ozonesondes (NILU, Norway). The Dutch-Finnish built OMI instrument is part of the NASA EOS Aura satellite payload. The OMI Project is managed by NIVR and KNMI in the Netherlands. Funding for this research was provided by NASA's Earth Science Mission.

References

Beer, R. (2006), TES on the Aura mission: Scientific objectives, measurements and analysis overview, *IEEE Trans. Geosci. Remote Sens.*, *44*, 1102–1105.

Bhartia, P. K. (2007), Total ozone from backscattered ultraviolet measurements, in *Observing Systems for Atmospheric Composition*, pp. 48–63, Springer, New York.

Bloom, S., et al. (2005), Documentation and validation of the Goddard Earth Observing System (GEOS) Data Assimilation System-Version 4, *Tech. Rep. Ser. on Global Model. and Data Assim. 104606*, NASA Goddard Space Flight Cent., Greenbelt, Md.

Chandra, S., J. R. Ziemke, and R. V. Martin (2003), Tropospheric ozone at tropical and middle latitudes derived from TOMS/MLS residual: Comparison with a global model, *J. Geophys. Res.*, *108*(D9), 4291, doi:10.1029/2002JD002912.

de Laat, A. T. J., I. Aben, and G. J. Roelofs (2005), A model perspective on total tropospheric O_3 column variability and implications for satellite observations, *J. Geophys. Res.*, *110*, D13303, doi:10.1029/2004JD005264.

Dessler, A. (2005), *The Chemistry and Physics of the Stratosphere*, 214 pp., Elsevier, New York.

Edwards, D. P., et al. (2003), Tropospheric ozone over the tropical Atlantic: A satellite perspective, *J. Geophys. Res.*, *108*(D8), 4237, doi:10.1029/2002JD002927.

21562202d, 2007, D24, Downloaded from https://agupubs.onlinelibrary.wiley.com/doi/10.1029/2007JD008773 by Spanish Cochrane National Provision (Ministerio de Sanidad), Wiley Online Library on [22/01/2026]. See the Terms and Conditions (https://onlinelibrary.wiley.com/terms-and-conditions) on Wiley Online Library for rules of use; OA articles are governed by the applicable Creative Commons License

Fishman, J., and J. C. Larsen (1987), Distribution of total ozone and stratospheric ozone in the tropics: Implications for the distribution of tropospheric ozone, *J. Geophys. Res.*, *92*, 6627–6634.

Fishman, J., C. E. Watson, J. C. Larsen, and J. A. Logan (1990), Distribution of tropospheric ozone determined from satellite data, *J. Geophys. Res.*, *95*(D4), 3599–3617.

Froidevaux, L., et al. (2006), Early validation analyses of atmospheric profiles from EOS MLS on the Aura satellite, *IEEE Trans. Geosci. Remote Sens.*, *44*, 1006–1121.

Kley, D., et al. (1996), Observations of near-zero ozone concentrations over the convective Pacific: Effects on air chemistry, *Science*, *274*, 230–232.

Kulawik, S. S., J. Worden, A. Eldering, K. Bowman, M. Gunson, G. B. Osterman, L. Zhang, S. A. Clough, M. W. Shephard, and R. Beer (2006), Implementation of cloud retrievals for Tropospheric Emission Spectrometer (TES) atmospheric retrievals: 1. Description and characterization of errors on trace gas retrievals, *J. Geophys. Res.*, *111*, D24204, doi:10.1029/2005JD006733.

Lelieveld, J., et al. (2002), Global air pollution crossroads over the Mediterranean, *Science*, *298*(5594), 794–799.

Levelt, P. F., et al. (2006), The Ozone Monitoring Instrument, *IEEE Trans. Geophys. Remote Sens.*, *44*, 1093–1101.

Liu, X., et al. (2006), First directly-retrieved global distribution of tropospheric column ozone from GOME: Comparison with the GEOS-CHEM model, *J. Geophys. Res.*, *111*, D02308, doi:10.1029/2005JD006564.

Livesey, N., et al. (2007), Validation of Aura Microwave Limb Sounder O_3 and CO observations in the upper troposphere and lower stratosphere, *J. Geophys. Res.*, doi:10.1029/2007JD008805, in press.

Martin, R. V., et al. (2002), Interpretation of TOMS observations of tropical tropospheric ozone with a global model and in situ observations, *J. Geophys. Res.*, *107*(D18), 4351, doi:10.1029/2001JD001480.

Marufu, L., et al. (2000), Photochemistry of the African troposphere: Influence of biomass burning emission, *J. Geophys. Res.*, *105*, 14,513–14,530.

Morris, G. A., J. F. Gleason, J. Ziemke, and M. R. Schoeberl (2000), Trajectory mapping: A tool for validation of trace gas observations, *J. Geophys. Res.*, *105*(D14), 17,875–17,894.

Moxim, W. J. (2000), A model analysis of tropical South Atlantic Ocean tropospheric ozone maximum: The interaction of transport and chemistry, *J. Geophys. Res.*, *105*, 17,393–17,415.

Randel, W. J., D. J. Seidel, and L. L. Pan (2007), Observational characteristics of double tropopauses, *J. Geophys. Res.*, *112*, D07309, doi:10.1029/2006JD007904.

Schoeberl, M., and L. C. Sparling (1995), Trajectory modeling, in *Diagnostic Tools in Atmospheric Physics*, edited by G. Fiocco and G. Visconti, *Proc. Int. Sch. Phys. Enrico Fermi*, *124*, 289–305.

Schoeberl, M. R. (2004), Extratropical stratosphere-troposphere mass exchange, *J. Geophys. Res.*, *109*, D13303, doi:10.1029/2004JD004525.

Schoeberl, M. R., et al. (2006), Overview of the EOS Aura Mission, *IEEE Trans. Geosci. Remote Sens.*, *44*, 1066–1074.

Thompson, A. M., K. E. Pickering, D. P. McNamara, M. R. Schoeberl, R. D. Hudson, J. H. Kim, E. V. Browell, W. J. H. V. Kirchhoff, and D. Nganga (1996), Where did tropospheric ozone over southern Africa and the tropical Atlantic come from in October 1992? Insights from TOMS, GTE/TRACE-A and SAFARI-92, *J. Geophys. Res.*, *101*, 24,251–24,278.

Thompson, A. M., et al. (2003), Southern Hemisphere Additional Ozonesondes (SHADOZ) 1998–2000 tropical ozone climatology: 1. Comparisons with Total Ozone Mapping Spectrometer (TOMS) and ground-based measurements, *J. Geophys. Res.*, *108*(D2), 8238, doi:10.1029/2001JD000967.

Thompson, A. M., et al. (2007), Intercontinental Chemical Transport Experiment Ozonesonde Network Study (IONS) 2004: 1. Summertime upper troposphere/lower stratosphere ozone over northeastern North America, *J. Geophys. Res.*, *112*, D12S12, doi:10.1029/2006JD007441.

Waters, J. W., et al. (2006), The Earth Observing System Microwave Limb Sounder (EOS MLS) on the Aura satellite, *IEEE Trans. Geosci. Remote Sens.*, *44*, 1075–1092.

Wimmers, A. J., and J. L. Moody (2004), Tropopause folding at satellite-observed spatial gradients: 1. Verification of an empirical relationship, *J. Geophys. Res.*, *109*, D19306, doi:10.1029/2003JD004145.

Worden, H. M. (2007), Comparisons of Tropospheric Emission Spectrometer (TES) ozone profiles to ozonesodes: Methods and initial results, *J. Geophys. Res.*, *112*, D03309, doi:10.1029/2006JD007258.

Ziemke, J. R., et al. (2006), Tropospheric ozone determined from aura OMI and MLS: Evaluation of measurements and comparison with the Global Modeling Initiative's Chemical Transport Model, *J. Geophys. Res.*, *111*, D19303, doi:10.1029/2006JD007089.

M. Allaart, H. Kelder, and P. F. Levelt, Royal Netherlands Meteorological Institute, NL-3730 De Bilt, Netherlands.

G. Ancellet and S. Godin-Beekmann, Service d'Aeronomie, Centre National de la Recherche Scientifique/Université Pierre et Marie Curie, F-75252 Paris, France.

S. B. Andersen, Danish Meteorological Institute, DK-2100 Copenhagen, Denmark.

P. K. Bhartia and M. R. Schoeberl, NASA Goddard Space Flight Center, Greenbelt, MD 20771, USA.

G. Bodeker, National Institute of Water and Atmospheric Research, Lauder, New Zealand.

B. Bojkov, S. Chandra, B. Duncan, S. Strahan, and J. R. Ziemke, Goddard Earth Sciences and Technology, University of Maryland, Baltimore County, Baltimore, MD 21228, USA.

B. Calpini, R. Stübi, and P. Viatte, Aerological Station Payerne, P.O. Box 316, MeteoSwiss, CH-1530 Payerne, Switzerland.

H. Claude, Meteorological Observatory Hohenpeißenberg, German Weather Service, Albin Schwaiger Weg 10, D-82383 Hohenpeißenberg, Germany.

G. Coetzee, Department of Environmental Affairs and Tourism, South African Weather Service, Private Bag X 97, Pretoria 0001, South Africa.

E. Cuevas and A. Redondas, Izana Observatory, National Institute of Meteorology, E-38071 Santa Cruz de Tenerife, Spain.

J. Davies and D. W. Tarasick, Environment Canada, Downsview, ON, Canada M3H 5T4.

H. de Backer, Royal Meteorological Institute of Belgium, Ringlaan 3, B-1180 Uccle, Belgium.

H. Dier, Meteorological Observatory Lindenberg, German Weather Service, Am Observatorium 12, D-15864 Lindenberg, Germany.

V. Dorokhov, Central Aerological Observatory, Pervomajskaya Street 3, Moscow 141700, Russia.

L. Froidevaux, S. Kulawik, and N. Livesey, NASA Jet Propulsion Laboratory, Pasadena, CA 91109, USA.

M. Fujiwara, Graduate School of Environmental Earth Science, Hokkaido University, Sapporo 060-0810, Japan.

G. Hansen, Norwegian Institute for Air Research, P.O. Box 1245, N-9001 Tromso, Norway.

B. J. Johnson and S. J. Oltmans, Global Monitoring Division, Earth System Research Laboratory, NOAA, Boulder, CO 80305, USA.

E. Joseph, Climate and Radiation Group, Howard University, Washington, DC 20059, USA.

G. Koenig-Langlo, Alfred Wegener Institute, Bussestrasse 24, D-27570 Bremerhaven, Germany.

E. Kyrö, Arctic Research Center, Finish Meteorological Institute, FIN-99600 Sodankyla, Finland.

C. P. Leong, Malaysian Meteorological Service, Jalan Sultan, Selangor 46667, Malaysia.

J. Merrill, Graduate School of Oceanography, University of Rhode Island, Narragansett, RI 02882, USA.

D. Moore, Met Office, Fitzroy Road, Exeter EX1 3PB, UK.

G. Morris, Department of Physics and Astronomy, Valparaiso University, Valparaiso, IN 46383, USA.

M. Newchurch, Atmospheric Science Department, University of Alabama-Huntsville, Huntsville, AL 46383, USA.

M. Parrondos and M. Yela, Laboratorio de Atmosfera, Spanish Space Agency, Cetra de Ajalvir km 4, E-27750 Madrid, Spain.

F. Posny, Laboratoire de Physique de l'Atmosphere de la Reunion, 15 Avenue René Cassin, BP 7151, F-97715 St Denis, Messag, Cedex 9, La Réunion, France.

F. J. Schmidlin, NASA Goddard Space Flight Center, Wallops Island, VA 23337, USA.

P. Skrivankova, Czech Hydrometeorological Institute, Na Sabatce 17, 14306 Prague, Czech Republic.

A. M. Thompson, Department of Meteorology, Pennsylvania State University, University Park, PA 16802, USA.

V. Thouret, Laboratoire d'Aerologie, CNRS, F-31400 Toulouse, France.

H. Vömel, Cooperative Institute for Research in Environmental Sciences, University of Colorado, Boulder, CO 80309, USA.

P. von der Gathen, Alfred Wegener Institute, D-14473 Potsdam, Germany.

J. C. Witte, Science Systems and Applications Inc., 10210 Greenbelt Road, Suite 600, Lanham, MD 20706, USA.

G. Zablocki, Centre of Aerology, National Institute of Meteorology and Hydrology, Zegrzynska 38, PL-05119 Legionowo, Poland.

21562024, 2007, D24, Downloaded from https://agupubs.onlinelibrary.wiley.com/doi/10.1029/2007JD008773 by Spanish Cochrane National Provision (Ministerio de Sanidad), Wiley Online Library on [22/01/2026]. See the Terms and Conditions (https://onlinelibrary.wiley.com/terms-and-conditions) on Wiley Online Library for rules of use; OA articles are governed by the applicable Creative Commons License